NOAA Technical Memorandum ERL SEL-75

THE TIROS - N / NOAA A-J SPACE ENVIRONMENT MONITOR SUBSYSTEM

R. A. Seale
R. H. Bushnell

Space Environment Laboratory
Boulder, Colorado
April 1987

UNITED STATES
DEPARTMENT OF COMMERCE

Malcolm Baldrige,
Secretary

NATIONAL OCEANIC AND
ATMOSPHERIC ADMINISTRATION

Anthony J. Calio,
Administrator

Environmental Research
Laboratories

Vernon E. Derr,
Director

NOTICE

Mention of a commercial company or product does not constitute an endorsement by NOAA Environmental Research Laboratories. Use for publicity or advertising purposes of information from this publication concerning proprietary products or the tests of such products is not authorized.

For sale by the National Technical Information Service, 5285 Port Royal Road
Springfield, VA 22161

CONTENTS

LIST OF FIGURES

LIST OF TABLES

The TIROS-N / NOAA A - J

SPACE ENVIRONMENT MONITOR SUBSYSTEM

R. A. Seale

Robert H. Bushnell

ABSTRACT. The Space Environment Monitor (SEM), which is incorporated as a subsystem in the TIROS-N and NOAA A-J satellites, is described. The SEM consists of a Total Energy Detector (TED), a Medium Energy Proton and Electron Detector (MEPED), a High Energy Proton and Alpha Detector (HEPAD) and a Data Processing Unit (DPU). The detectors are intended to provide near real time particle data for use in the Space Environment Service Center of NOAA and to provide a long term scientific data base. Telemeter codes, data reduction, and test instructions are given.

Key Words: Polar Orbiting Satellite, particles, monitoring, space.

1. INTRODUCTION

The objective of this report is to bring together in convenient form all the information on the SEM pertinent to use of the data and understanding its operation. The TIROS-N Space Environment Monitor (SEM) makes measurements of the Earth's charged particle environment. The data from the SEM detectors are used operationally by the Space Environment Services Center (SESC) of the US National Oceanic and Atmospheric Administration (NOAA) in Boulder, Colorado. The SESC, which is operated jointly by NOAA and the USAF Air Weather Service, has the US national responsibility for the preparation and dissemination of monitoring and forecasting information on solar activity and the state of the Earth's space environment, and the effects of these on man's activities. In addition, it is designated as the World Warning Agency by the International Union of World Data Centers (IUWDC). Affected activities are as diverse as the scheduling of geophysical surveying using the Earth's magnetic field, the planning of scientific experiments and the reduction of data from such experiments; to the radiation hazards to people in space or, during occasional giant solar particle events, to passengers and crew of high flying aircraft on polar routes.

The TIROS-N polar orbit affords the opportunity to make direct measurements of phenomena at high latitudes where the Earth's magnetic field geometry permits the free access of charged particles to the polar cap areas surrounding each magnetic pole, and to the region where particles trapped in the outer magnetosphere can be precipitated into the Earth's atmosphere during magnetic disturbances.

The TIROS-N SEM was provided by Ford Aerospace and Communications Corp. (FACC) as a subcontractor to the Space Environment Laboratory. A list of the major individuals involved is given in the acknowledgments. Much of the graphic material is from contractors' publications.

2. SPACECRAFT AND SEM

The TIROS-N/NOAA-A-G spacecraft, shown in Figures 1 and 2, is a five-sided box-like structure which is 3.71 meters long and 1.88 meters in diameter. Four of the side faces are equal in size and accommodate thermal control louvers in each face. The fifth side is wider than the other four to accommodate the earth-facing communications antennas and some of the earth viewing sensors. The spacecraft has a mass of 1421 kg at launch including expendables.

At one end of the central body known as the Equipment Support Module is the Reaction Support Structure which includes the last stage launch injection motor, an attitude control propulsion system and a boom-mounted solar cell array. The 11.6 sq. meter solar array is motor driven to rotate once per revolution in orbit so that it will continuously face the sun during the daylight portion of the orbit.

The Manipulated Information Rate Processor (MIRP) processes the high rate data from the Advanced Very High Resolution Radiometer (AVHRR) in order to

provide separate, real time outputs for Automatic Picture Transmission (APT) and High Resolution Picture Transmission (HRPT), recorded Global Area Coverage (GAC) of reduced resolution data and recorded Local Area Coverage (LAC) of high resolution data. By command these are read out at the CDA's and processed in the NOAA central computer facility at Suitland, Maryland. The four data formats are put out simultaneously. LAC is similar to the recorded HRPT data of the ITOS system known as VREC.

In addition to formatting, the MIRP adds synchronization, identification, time code, telemetry and the TIROS Information Processor (TIP) output to the AVHRR data. The high resolution AVHRR is reduced in resolution by averaging techniques for use in the APT and GAC formats. The HRPT and LAC are put out from the MIRP at 0.66 megabits per second while the APT is in analog form.

ADVANCED VERY HIGH RESOLUTION RADIOMETER.

The instrument data which are processed by the TIP include the TIROS Operational Vertical Sounder (TOVS), the Space Environment Monitor (SEM), and the Data Collection System (DCS). NOAA-F and -G have been designated Advanced TIROS N (ATN) and have a somewhat different complement of instruments which varies with the particular spacecraft. A Search and Rescue (SAR) receiver is included.

The individual instrument data rates going into the TIP are as follows:

HIRS/2	2880	bits	per	second
SSU	480	"	"	"
MSU	320	"	"	"
SEM	160	"	"	"
DCS	720	"	"	"

The TIP data are put out as one channel of serial digital words at 8320 bits per second included in the real time beacon transmission and recorded data.

The NOAA-A SEM consists of three detector and analog electronics sections which feed a common Data Processing Unit (DPU). The three SEM detectors, a Total Energy Detector (TED), a Medium Energy Proton and Electron Detector (MEPED) and a High Energy Proton and Alpha Detector (HEPAD), measure the flux and spectrum of charged ambient particles at the spacecraft. In addition, the TED and, in the low energy portion of its range, the MEPED measure two points on the spatial distribution function by having two detectors make directional measurements at different angles to the geomagnetic field.

The division of the detectors into the three groups reflects the three different detector technologies used to cover the wide energy range between 300 eV and 850 MeV. Figure 3 and Figure 4 show the outputs of the SEM.

The three SEM sensors are shown in Figure 2. The DPU is located inside the Equipment Support Module and is therefore not visible.
The mass of each, less cables, is:
TED 3200 g, MEPED 3200 g, HEPED 3300 g, DPU 3100 g; total 12800 g.

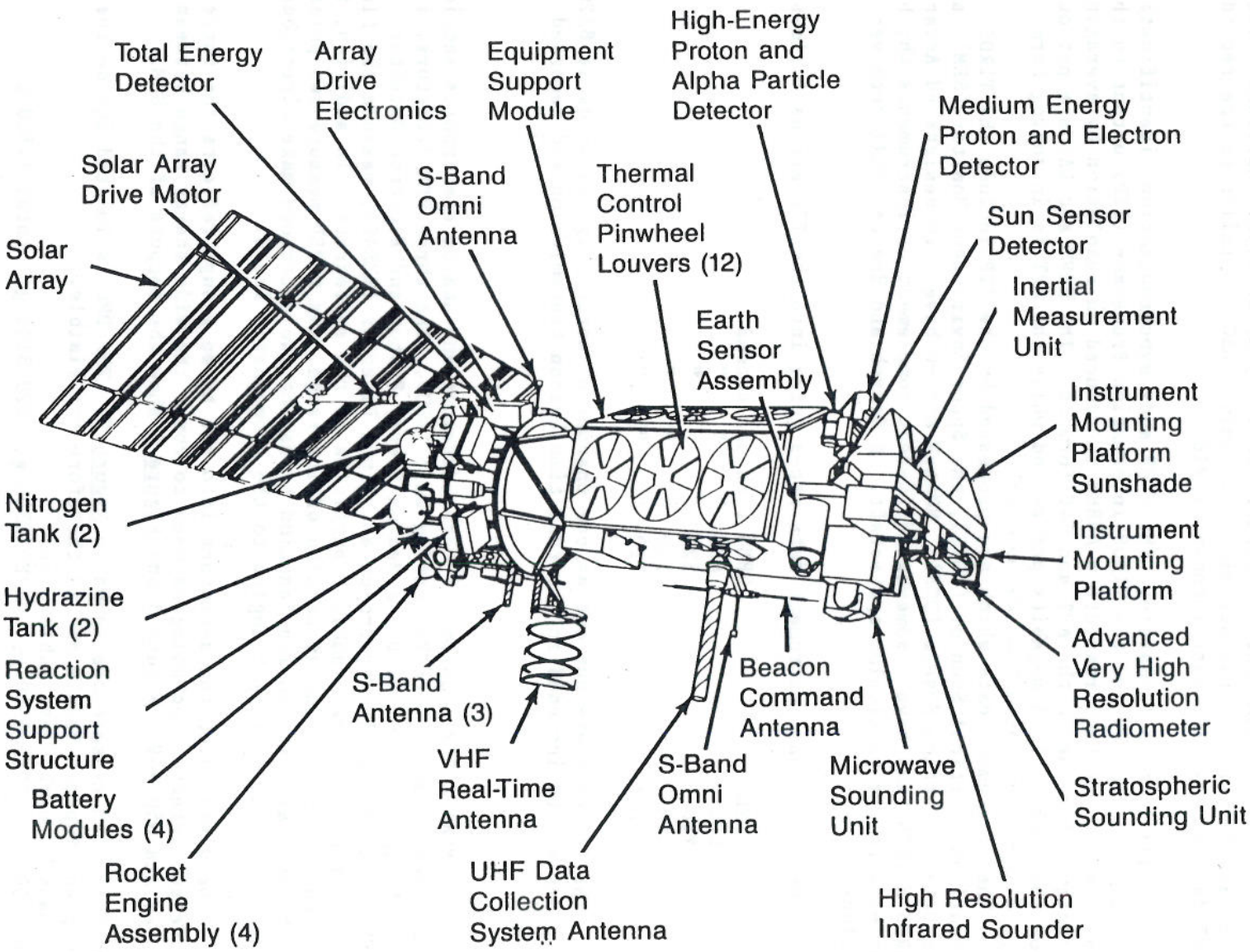

Figure 1.—TIROS–N Spacecraft Diagram

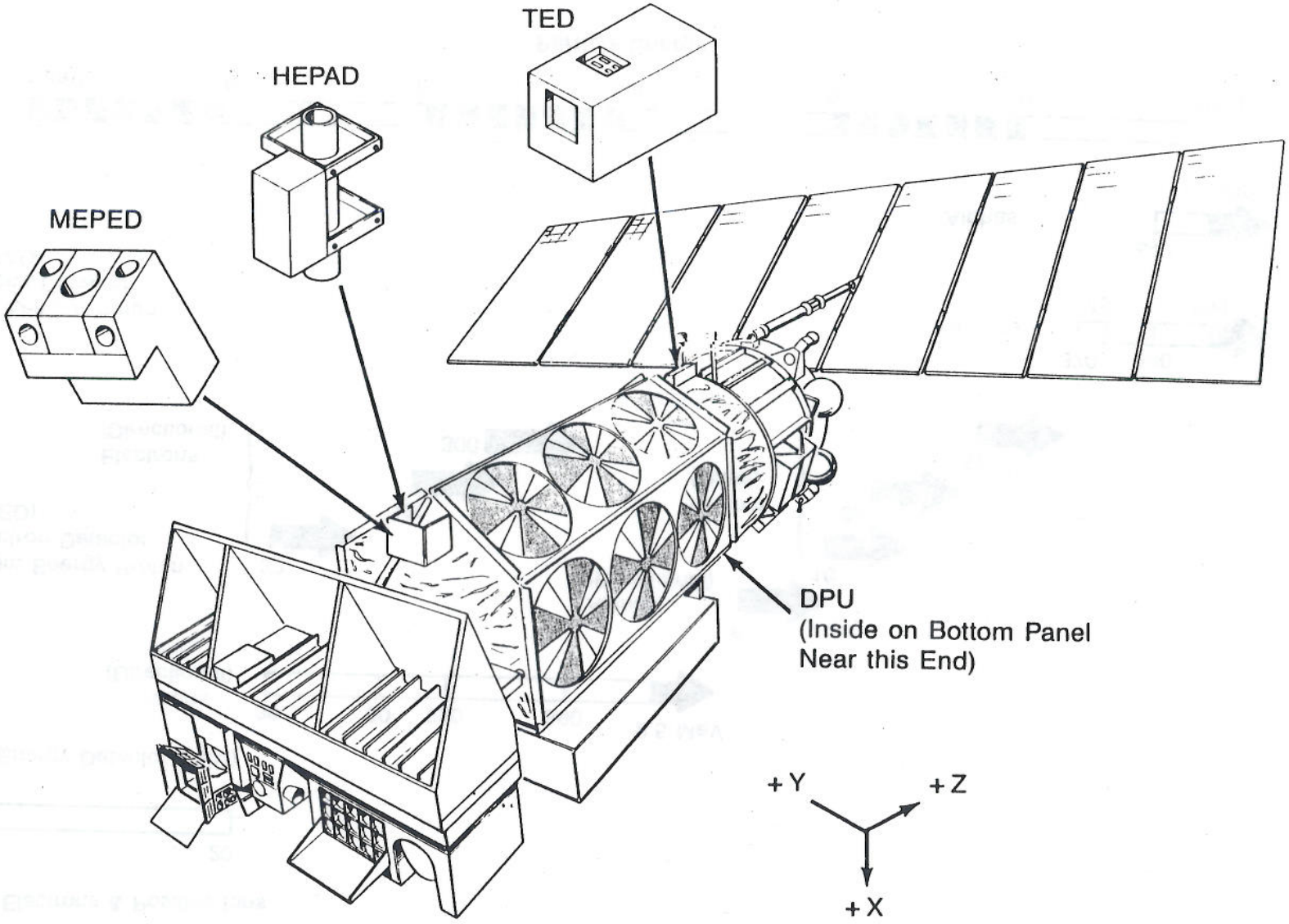

Figure 2.—SEM on TIROS-N

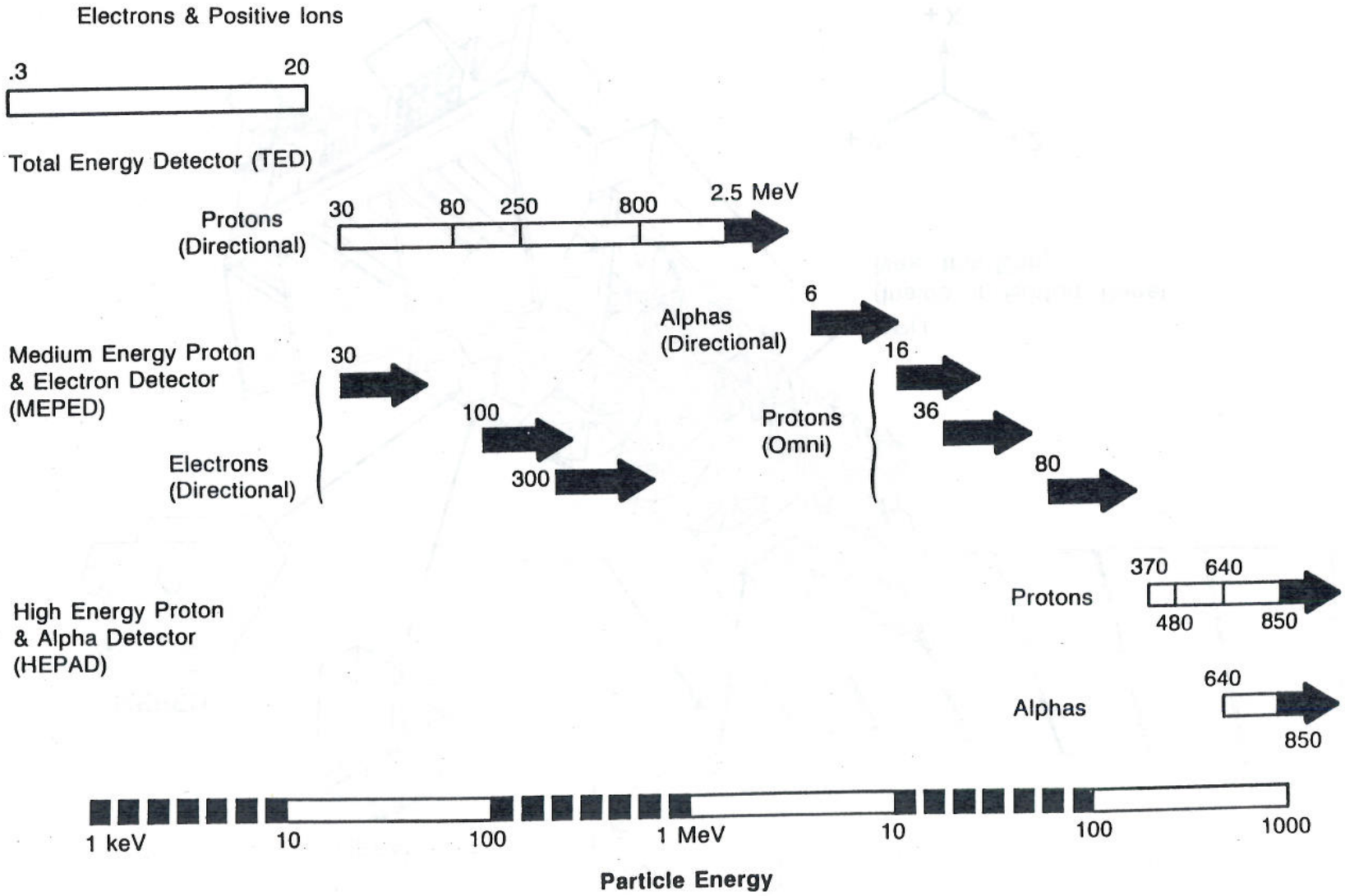

Figure 3.—Energy Coverage of the TIROS-N Space Environment Monitor

	Data Channel	Particle Type	Energy Range	Field of View		Max. Counting Rate pps	Data Sampling Interval	Other
				Aperture Axis	Cone Half Angle			
TED	$F_D(\alpha).(DE)_m.E_m$	Electrons	0.3-20 Kev	0°(Zenith)	~3°	$4x10^5$	2 sec	$F_D(\alpha)$ accuracy: ±50% $(DE)_m$ accuracy: ±50% E_m accuracy: ±30% Resolution: Statistical in weak fluxes <±6% in strong fluxes Insensitive to sunlight, moonlight. IFC: Preserves 7 1/2% accuracy.
	"	Protons	"	"	"			
	"	Electrons	"	30°	"			
	"	Protons	"	"	"			
	$(DE)_{1,3,5,7}$	E,P	Four Differential	0°,30°	"		4 or 8 sec	
MEPED Telescopes	P_1 P_2 P_3 P_4 P_5	Protons	30-80 Kev 80-250 Kev 250-800 Kev 800-2.5 Mev >2.5 Mev	0° (Zenith)	14°	$5x10^7$	2 sec	Noise Resolution: 7 Kev FWHM tele. 60 Kev FWHM OMNI Telescopes insensitive to incorrect particle type Energy Interval Stability: <±20% at $5x10^5$ counting rate IFC: Provides energy intervals; " noise resolution in telescopes Lifetime: Operation within specification for 5 years for all channels except P1 and E1.
	Same as above box	Protons	Same as above box	90°	"			
	E_1 E_2 E_3	Electrons	>30 Kev >100 Kev >300 Kev	0°	"			
	Same as above box	Electrons	Same as above box	90°	"			
	$0^1 90^1$	Positive Ions ($Z \geq 2$)	>6 Mev	0°,90°	"	Not Specified	16 sec	
MEPED OMNI	P_6 P_7 P_8	Protons	>16 Mev >36 Mev >80 Mev	0° (Zenith)	60°	$2x10^5$	2 sec	
HEPAD	P_1 P_2 P_3 P_4	Protons	370-480 Mev 480-640 Mev 640-850 Mev >850 Mev	0° (Zenith)	24°	$7x10^4$	4 sec	Accuracy: <±20% in count rate and energy intervals. IFC: Verifies accuracy specifications
	α_1 α_2	Alpha Particles	640-850 Mev/Nucleon >850 "	" "	"	10^4		
	$S_1 S_2 S_3$ S_5 S_4	All P, α $Am^{241}\alpha$	All >65 Mev/Nucleon ~5.4 Mev	– 0° (Zenith) –	180° 24° –	$2x10^5$		

Figure 4.—Performance Requirements

3. TOTAL ENERGY DETECTOR (TED)

3.1 General Description

The TED measures electrons and positive ions (often assumed to be protons) in the energy range 300 eV to 20 keV. Four separate detector assemblies measure the negatively charged and positively charged particles, respectively, at two angles; one approximately parallel to the magnetic field at high latitudes and the other at 30° to the first. Figure 5 shows a general view of the TED.

The detector assembly (Figure 6) uses a cylindrical-plate electrostatic analyzer with approximately a 13% energy resolution. A voltage difference is impressed on the analyzer plates. The polarity of this voltage determines whether positively charged ions (assumed always to be protons) or negatively charged particles (assumed to be electrons) are detected. The magnitude of this voltage selects a band of particle energies centered at some energy E for which the particles are passed through the analyzer.

The analyzer is followed by a "spiraltron" type channel electron multiplier (called a channeltron in Figure 7) which produces a relatively large pulse of electrons for input particles of either positive or negative charge, independent of the original particle energy. It does this in an electron avalanche (regardless of the charge or species of the input particle) of secondary emission. Preacceleration fields of appropriate polarity are applied between the electrostatic analyzer exit and the spiraltron cathode to ensure that even the lowest energy particles produce enough electrons at the cathode surface to be counted. The channel electron multiplier counts those charged particles which have passed through the analyzer.

A block diagram of the TED detector and analog electronics is shown in Figure 7. The basic signal chain between the detector spiraltrons and the logic pulse output to the DPU consists of linear amplification and pulse shaping followed by a "level comparator". There are four "levels" in the level comparator, set by the two attenuator levels and by the two reference levels shown at the right side of Figure 7. Two signal chains are used which are multiplexed sequentially between the detectors at 0° and those at 30°. See p. 91 for commands for these levels.

To allow for the loss of electron multiplication gain which occurs over the lifetime in orbit (basically a function of the number of events detected) the channeltron gain can be adjusted by varying its high voltage power supply (HVPS); 8 voltage steps are provided for this purpose. To determine the correct setting, a crude distribution of pulse heights from each detector is obtained by calibrating with the four comparator levels. Provision is made for this automatic "In-Flight Calibration" (IFC) under control of a sequence generated by the DPU which is started by ground command.

Four separate but identical analyzers, mounted in pairs, are included in the TED. Each pair views charged particles coming from different directions so that observations can be made of the directional energy flux at two different angles to the local geomagnetic field direction. One pair of

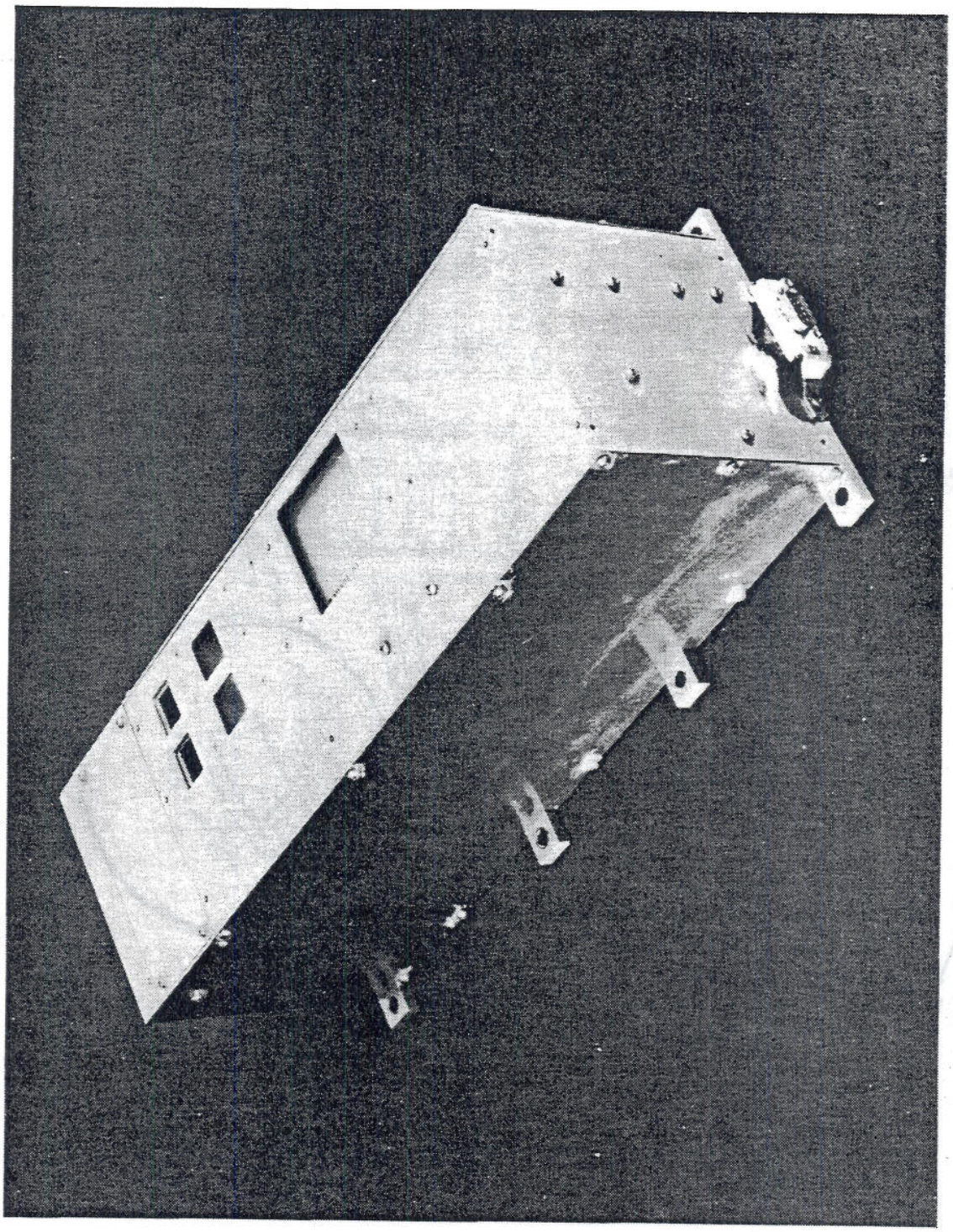

Figure 5.—Total Energy Detector

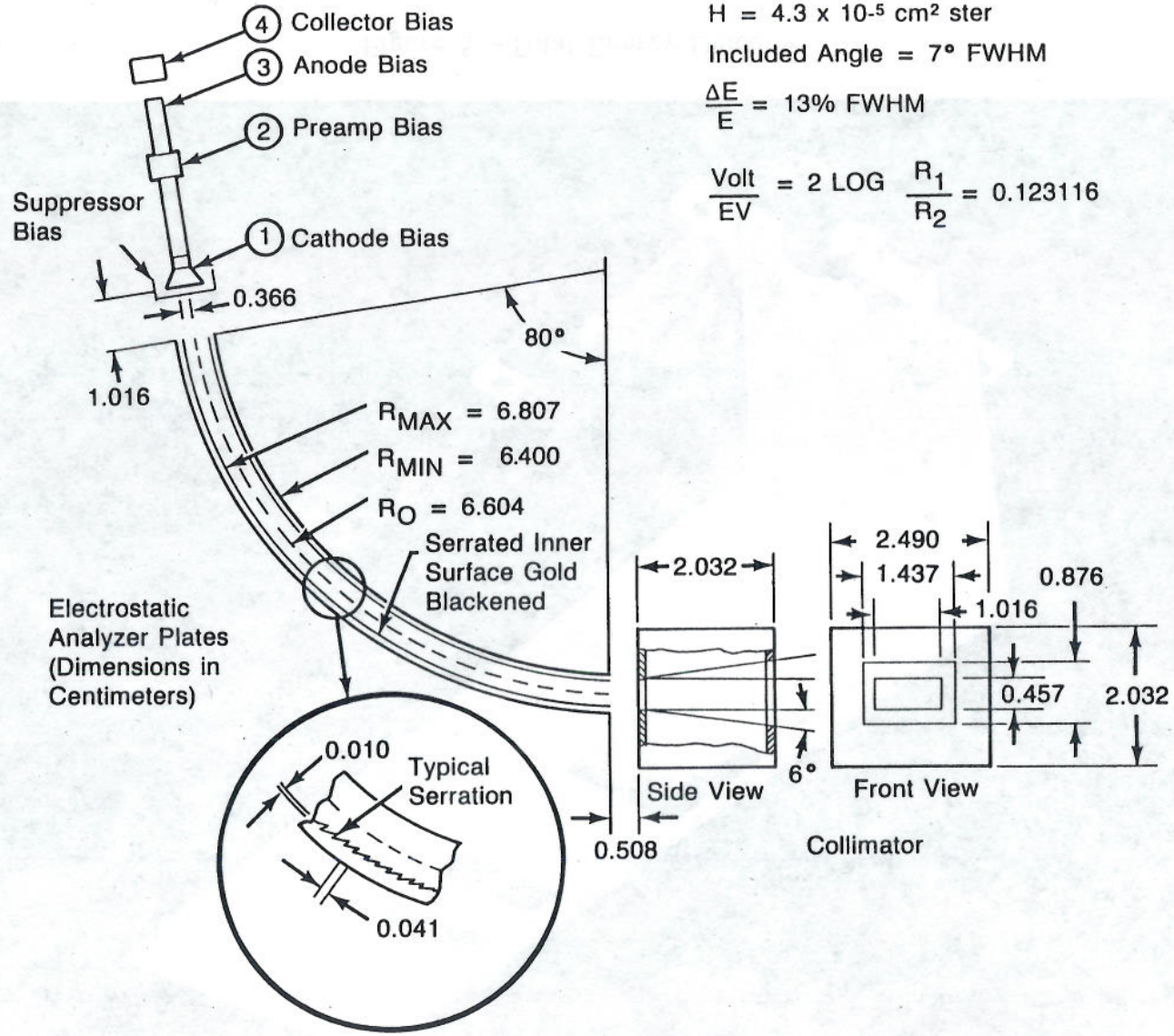

Figure 6.—TED Analyzer

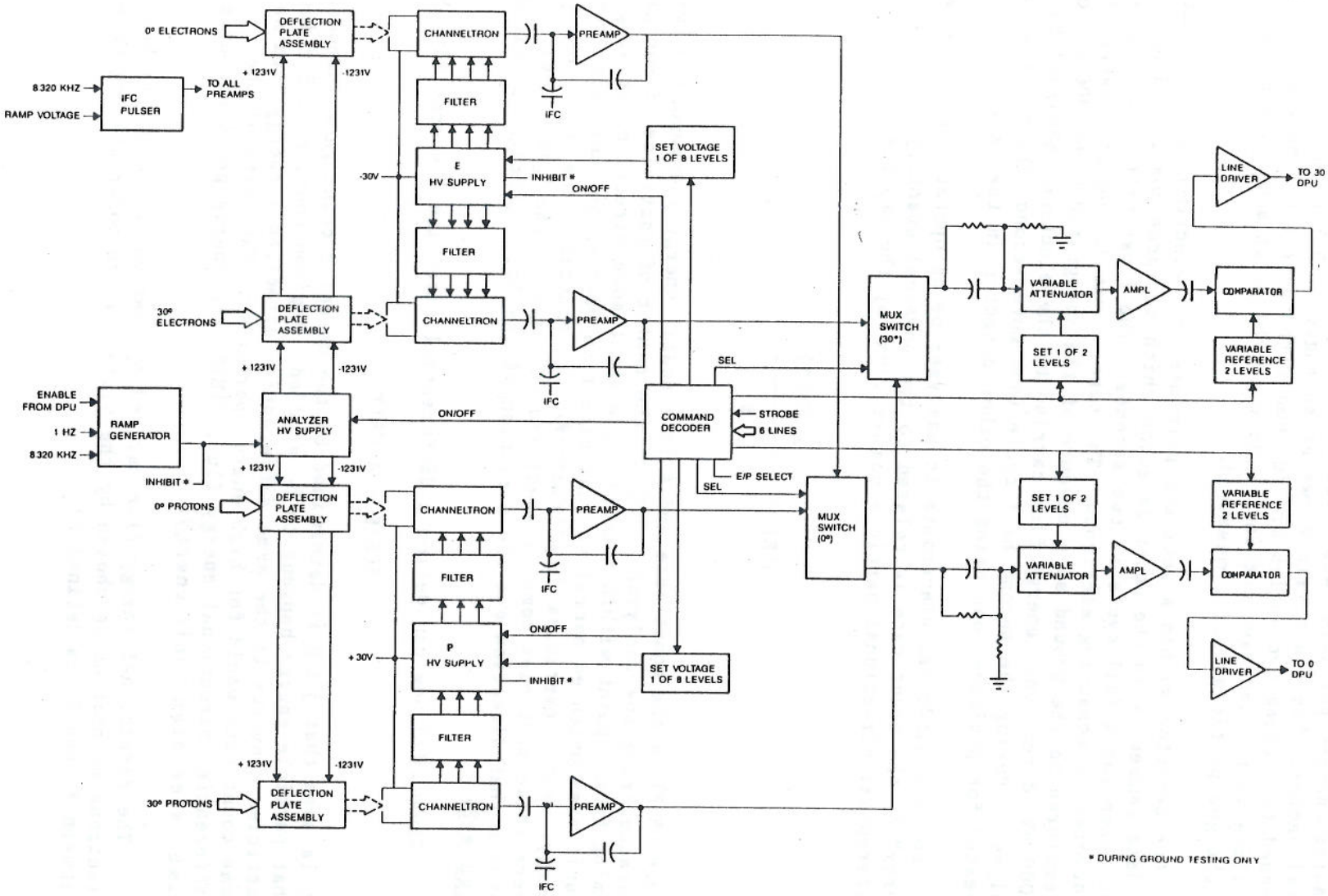

Figure 7.—TED Block Diagram

detectors views outwards parallel to the earth-center radial vector so that it measures charged particles whose velocities are toward the earth along this radial vector. The other pair views at an angle of 30^{o} from the first. It is stressed that these two angles are defined with respect to the earth-center satellite vector and have nothing to do with the pitch angle α associated with the charged particles being measured.

One detector within a detector pair measures electrons and alternates in the data segment with the other detector which measures positive ions. The time taken for a full cycle is two seconds. The first half cycle (one second) is devoted to measuring electrons. The total count during this sweep is telemetered to the ground as a measure of the integrated (from 300 eV to 20,000 eV) directional energy flux carried by the electrons observed by that analyzer. During the second half cycle (one more second) the process is repeated for positive ions using the other detector in the pair.

For a cylindrical electrostatic analyzer being operated at a "center energy" E, the count rate is related to the physical quantity j(E), the differential directional particle number flux, by the expression

$$j(E) = \frac{A\ CR(E)}{E}$$

where CR(E) is the count rate and A is a nearly energy-independent number characterizing the analyzer. j(E) is the number of particles of energies E, coming from a point within a solid angle about some direction, passing through a unit area oriented normal to that direction vector, per unit time per unit energy; units: particles /($cm^2 \cdot s \cdot sr \cdot keV$). In practice, the direction from where these particles come is specified in terms of the "pitch angle" between that direction and the direction of the local geomagnetic field (see Figure 8).

Given j(E) one can define a differential directional energy flux by

$$j(E)E = A\ CR(E).$$

It is seen that j(E)E is determined by the detector count rate independent of what particle energy happens to be studied. A given count rate for low energy particles converts to the same differential directional energy flux as the same count rate would for high energy particles. The units of the differential directional energy flux, j(E)E, are energy per (unit area · unit time · steradian · unit energy).

The directional energy flux carried by charged particles (either electrons or protons as chosen by the plate voltage polarity) having energies between E_1 and E_2 is defined by

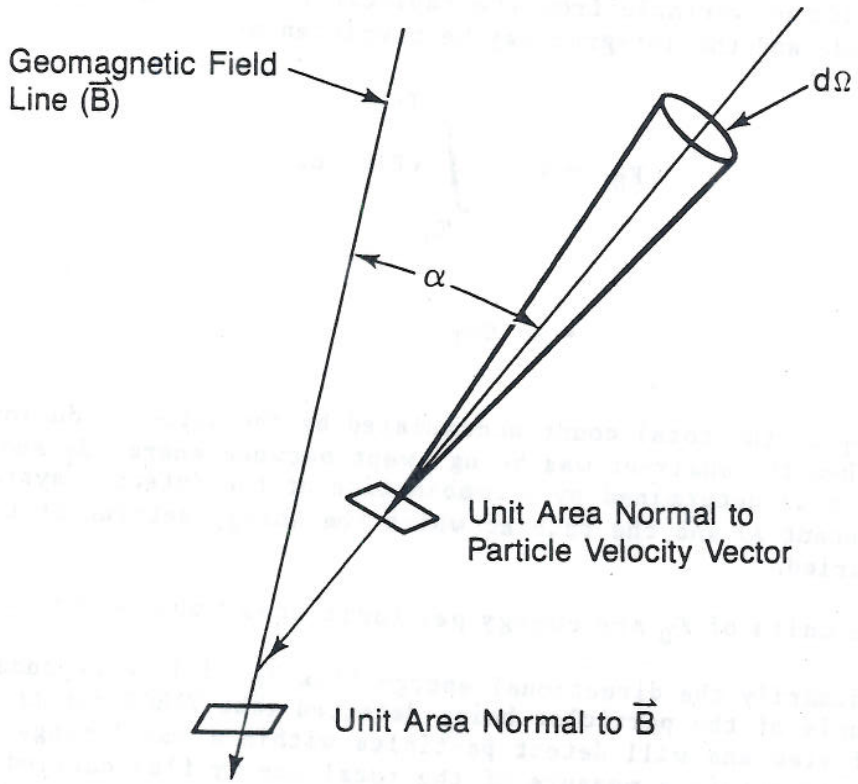

Figure 8.—Particle Pitch Angle α

$$F_D = \int_{E_1}^{E_2} j(E)\, E\, dE$$

$$= \int_{E_1}^{E_2} A\, CR(E)\, dE$$

Here the detector count rate CR(E) is shown as an explicit function of the particle energy E which, in turn, is directly proportional to the voltage between the analyzer plates. If this plate voltage is varied linearly with time from measuring charged particles of energy E_1 to particles of energy E_2, then a shift of variable from the explicit E to the implicit variable t (time) may be made and the integral may be rewritten as

$$F_D = k \int_{T_1}^{T_2} CR(t)\, dt$$

$$= k\ CR_T$$

where CR_T is the total count accumulated by the detector during the time period when the analyzer was being swept between energy E_1 and E_2. The constant k is determined by a combination of the detector system sensitivity (the constant A) and the rate at which the energy setting of the analyzer is being varied.

The units of F_D are energy per (unit area · unit time · steradian).

Ordinarily the directional energy flux F_D will be dependent upon the pitch angle of the particles being detected (the TIROS detector has a small field of view and will detect particles within a small range of pitch angle). In order to obtain a measure of the total energy flux carried by these particles through a unit area oriented normal to the geomagnetic field B, F_D must be integrated over the pitch angle α.

If F_D is known as a function of α at the top of the atmosphere, normally taken to be 120 km altitude, then the energy flux through a unit area normal to B will be

$$F_T = 2\pi \int_0^{\pi/2} F_D(\alpha)\, \sin\alpha \cos\alpha\, d\alpha$$

The units of F_T are energy per (unit area · unit time).

For all latitudes relevant to the TIROS observations (i.e. poleward of 40 degrees latitude) the inclination of B to the horizontal is greater than 60°.

Thus, identifying the energy flux through a unit area normal to B with the actual energy flux into the atmosphere will introduce an error of no more than (1 - cos 30) which is 15%.

The prime function of the TIROS-N instrument is to measure the directional energy flux F_D for each of the two particle species, electrons and protons, at each of two pitch angles. This is sufficient to estimate the total energy fluxes F_T for each of the particle species and the sum of these two energy fluxes.

While the main output of the TED, as its name implies, is the total incident energy flux, the electrostatic analyzer sorts particles by their charge and energy. The energy flux measurement is accomplished by sweeping the analyzer voltage in synchronism with the data processing and telemetry in the DPU. The total flux is formed by adding up the sorted counts.

For simplicity of ground processing and to minimize telemetry requirements, this sum is done in the SEM by sweeping the electrostatic analyzers with a piecewise linear ramp voltage. Figure 9 shows some details of the sweep. Measurements of a single particle species are made over a 1-second period. The 1-second period is split into 13 equal intervals. Background (particle count) is measured over the first interval (78 ms), when the ramp voltage applied to the electrostatic analyzer is set to zero. The energy sweep from 300 eV to 20,000 eV takes 11/13 second. Counts are accumulated during each successive 1/13 s interval for 11 intervals. There is one interval at the end to allow the ramp voltage to reset.

During the sweep of the 11 intervals a 5-bit binary prescaler is reduced by factors of two in synchronism with increases in the slope, which is also changed by factors of two, of the piecewise linear ramp voltage, so as to weight each contribution to the final accumulated count in proportion to its energy content, thus arriving at the total energy.

Of the 11 values generated by a single detector during an energy sweep, four are telemetered every fourth sweep. The four represent the counts accumulated during intervals 2, 4, 6, and 8 corresponding to energy bands 1, 3, 5, and 7.

An additional piece of information derived for each sweep is the energy band number containing the highest count thus giving an indication of the predominant energy in the incident spectrum. This is done so that an estimate can be made as to what energy particles are carrying the bulk of the energy flow and, thus, what altitude in the atmosphere this energy is ultimately deposited. Part of this information is telemetered at a slower rate in submultiplexed words.

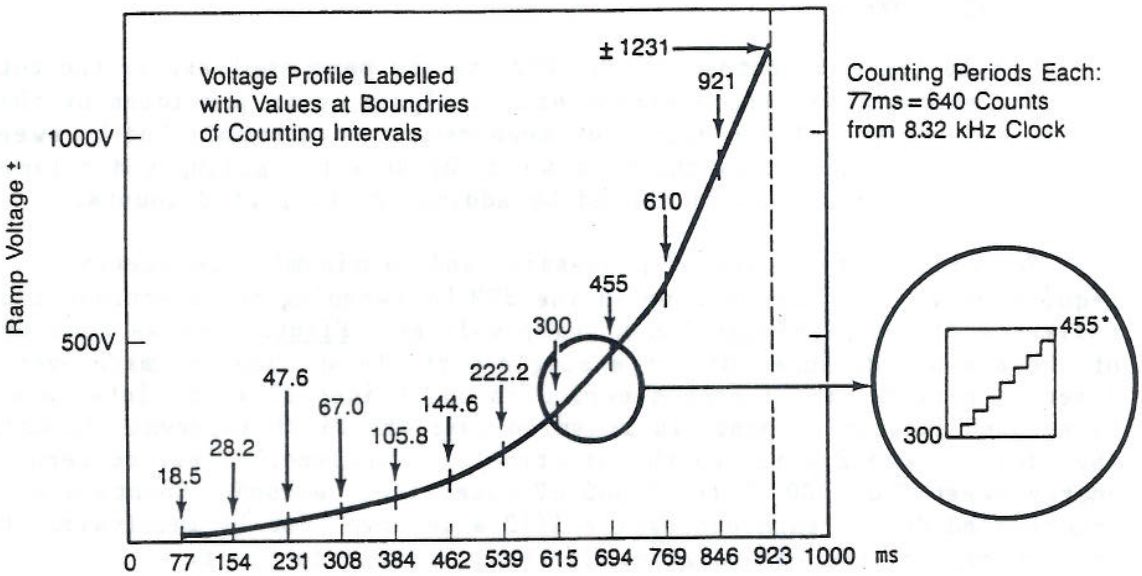

Channel Energy (Kev)	Ramp Range (V)	Energy Interval (Kev)			Data Channel Label	Number of Pre-Scaling Bits in F_D (a) comp
		Width	Center	Width Center		
0	0	—	—	—	BKGND	—
0.300- 0.458	18.5- 28.2	0.158	0.379	0.42	DE 1	5
0.458- 0.773	28.2- 47.6	0.315	0.616	0.51	DE 2	4
0.773- 1.088	47.6- 67.0	0.315	0.931	0.34	DE 3	4
1.088- 1.718	67.0- 105.8	0.630	1.403	0.45	DE 4	3
1.718- 2.349	105.8- 144.6	0.630	2.033	0.31	DE 5	3
2.349- 3.610	144.6- 222.2	1.261	2.979	0.42	DE 6	2
3.610- 4.870	222.2- 299.8	1.261	4.250	0.30	DE 7	2
4.870- 7.392	299.8- 455.0	2.522	6.131	0.41	DE 8	1
7.392- 9.914	455.0- 610.2	2.522	8.653	0.29	DE 9	1
9.914-14.957	610.2- 920.6	5.043	12.436	0.41	DE10	0
14.957-20.000	920.6-1231.0	5.043	17.479	0.29	DE11	0
0.300-20.0	18.5-1231.0				F_D (a)	

Ramp Characteristics

Figure 9.—TED Ramp Characteristics

The count accumulated during a single subinterval of the energy sweep relates to the directional energy flux within the limited energy range swept by the detector in the 1/13-second subinterval. By dividing this directional energy flux by the width of the energy band sampled, the directional differential energy flux at the center energy of the band may be obtained.

Table 1 lists the details of each of these 11 energy bands.

TABLE 1. ENERGY BANDS OF THE TED

Energy Band #	Edges of Band (eV)	Center Energy (eV)	Conversion from Count to Directional Energy Flux (ergs/(cm^2·s·sr))		Altitude at Which Energy is Deposited km
			electrons	protons	
1	300- 458	379	5.97×10^{-5}	4.69×10^{-5}	>300
2	458- 773	616	1.19×10^{-4}	9.38×10^{-5}	215
3	773- 1088	931	1.19×10^{-4}	9.38×10^{-5}	190
4	1088- 1718	1403	2.38×10^{-4}	1.88×10^{-4}	165
5	1718- 2349	2033	2.38×10^{-4}	1.88×10^{-4}	145
6	2349- 3610	2979	4.76×10^{-4}	3.75×10^{-4}	130
7	3610- 4870	4250	4.76×10^{-4}	3.75×10^{-4}	120
8	4870- 7392	6131	9.52×10^{-4}	7.50×10^{-4}	115
9	7392- 9914	8653	9.52×10^{-4}	7.50×10^{-4}	108
10	9914-14957	12436	1.90×10^{-3}	1.50×10^{-3}	105
11	14957-20000	17479	1.90×10^{-3}	1.50×10^{-3}	104

The telemetered number is multiplied by the conversion factor to obtain the desired quantity in physical units.

3.2 Calibration for the TED

Calibration data are contained in the End Item Data package prepared for each SEM by the manufacturer, Ford Aerospace and Communication Corporation (FACC) which gives the results of instrument calibration performed at the low-energy particle calibration facility at Rice University.

The conversions between these telemetered values and the corresponding directional energy flux in physical units are given in Table 2. The difference in conversion between electrons and protons reflects a difference in detection efficiency for the two particle species.

TABLE 2. TED CONVERSION FROM TELEMETERED VALUES

Directional Energy Flux ergs/($cm^2 \cdot s \cdot sr$) per count	
Electrons:	1.905×10^{-3} x 0EFD or 30EFD
Protons:	1.50×10^{-3} x 0PFD or 30PFD

Directional Energy Flux in Each Band erg/($cm^2 \cdot s \cdot sr \cdot eV$) per count at the center energy	
Electrons	3.78×10^{-7}
Protons	2.97×10^{-7}

3.3 TED Data

The following are the data obtained by the TED, their meaning, and the frequency/timing with which they are obtained.

0EFD, 30EFD 0PFD, 30PFD	The TED directional count from each of two pitch angles for each of the two particles species at the location of the satellite. These numbers are proportional to the directional energy flux between 300 eV and 20 keV. The full set of four values is transmitted continuously every two seconds (about 15 km of spacecraft travel).
Total Energy	The total energy flux into the atmosphere at 120 km as computed from the four individual directional measurements every two seconds.
0DEM, 0EM 30DEM, 30EM 0DPM, 0PM 30DPM, 30PM	The energy channel number EM or PM within which the maximum count rate was observed together with the value DEM or DPM of that count rate. This data set is transmitted continuously every two seconds.

0DE1, 0DE3 0DE5, 0DE7 30DE1, 30DE3 30DE5, 30DE7	These four sets of differential directional energy flux values for energy bands 1, 3, 5 and 7 (sweep intervals 2, 4, 6 and 8) are transmitted in a sequence requiring 8 seconds. These data appear only in record types 1, 2 and 3. Record type means one of the four 8-second parts of the 32-second telemeter period listed in Appendix H.
0DP1, 0DP3 0DP5, 0DP7 30DP1, 30DP3 30DP5, 30DP7	
0EBK, 30EBK 0PBK, 30PBK	The count accumulated during the first 1/13 second (background interval) of each of 16 energy sweeps associated with labeled detector and particle species. These data are transmitted every 32 seconds and appear in output record type 4 only.

The four observations (0EFD, 30EFD, 0PFD, and 30PFD), which constitute a measure of the total energy, are the prime data from the TED instrument and are transmitted continuously every two seconds (about 15 km of spacecraft travel).

Because there are four detectors there are a total of four directional data sets (or 16 points) available every two seconds. Only one in four such sets are actually transmitted, the sequence being:

first two seconds	0DE1, 0DE3, 0DE5, 0DE7
next two seconds	30DE1, 30DE3, 30DE5, 30DE7
next two seconds	0DP1, 0DP3, 0DP5, 0DP7
last two seconds	30DP1, 30DP3, 30DP5, 30DP7

The data channel identification here includes the detector direction (0 or 30), the particle species (E or P) and the energy band (1, 3, 5, 7).

3.4 TED Data Interpretation

All these physical variables listed so far are those measured at the satellite at 850 km altitude. These measured values are manipulated, together with a geomagnetic field model (IGRF) to obtain the truly relevant variable: the magnitude of the energy flow into the atmosphere and the location at which this energy input is occurring.

Figure 10 illustrates this situation. Charged particles measured at the satellite are guided along the magnetic field lines. Because these magnetic lines of force are not radial, the point at which the field line passing through the satellite intersects the atmosphere may be displaced considerably from the subsatellite point. The magnetic field model is used to trace the field line passing through the satellite to the point where the field line intersects the atmosphere at 120 km. (This point is called the "foot of the

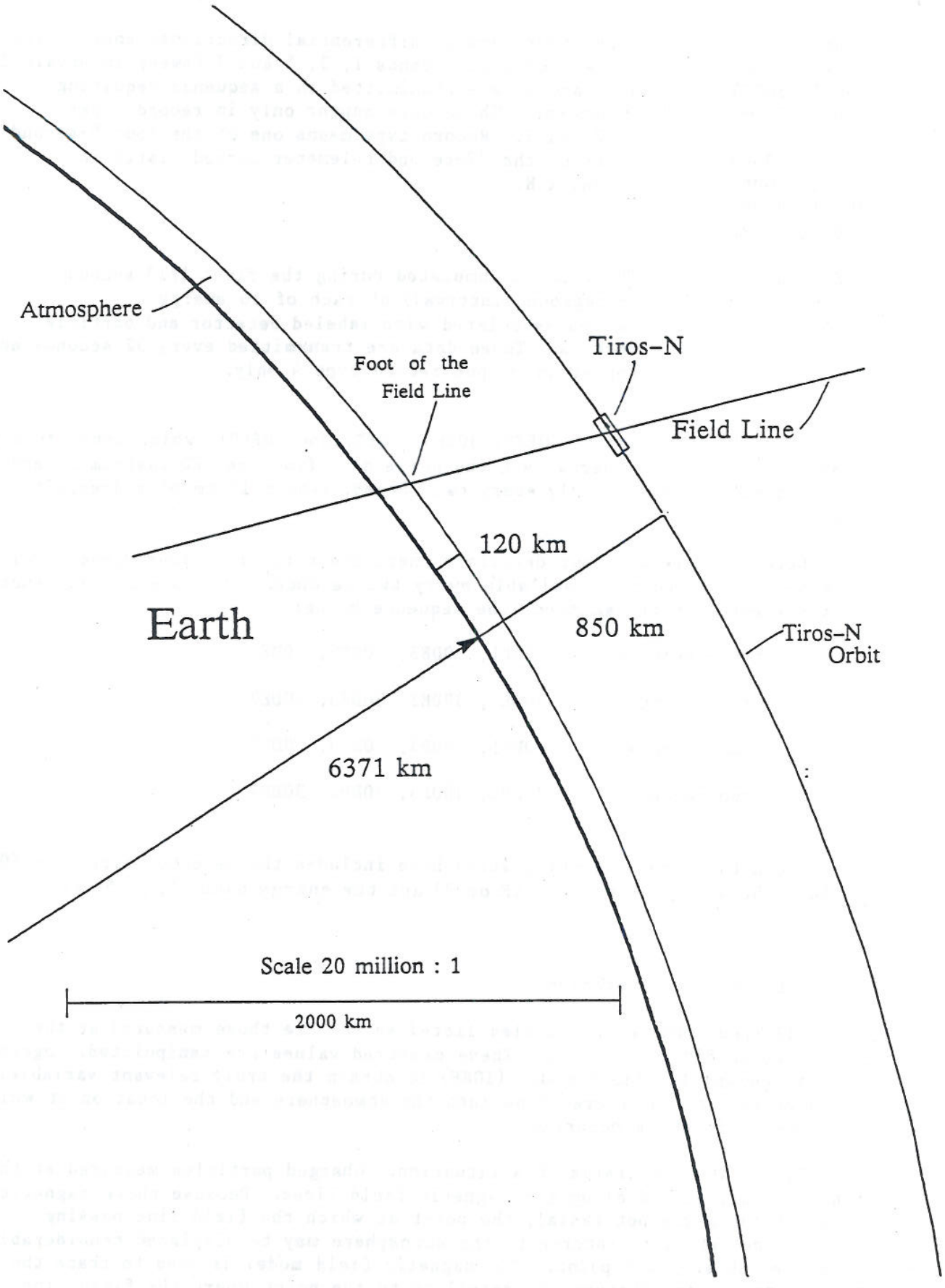

Figure 10.—Relationship Between Field Lines and Spacecraft

field line", FOFL). The co-ordinates of this point, both geographic and geomagnetic, together with the solar time and magnetic time are calculated and given in the header records of an archive tape made for all data. Zero of magnetic time occurs when the sun crosses the lower branch of the meridian through the geographic pole and the northern magnetic pole. By convention, if TIROS-N is north of the geomagnetic equator, the FOFL is taken to be in the northern hemisphere. Otherwise the FOFL is in the southern hemisphere.

The angles between the geomagnetic field direction and the look direction of the two detectors are also computed using the geomagnetic field model. These two angles are the local pitch angles of the charged particles being studied by the two detectors. However, because of the "magnetic mirror effect" on the motion of charged particles, the pitch angles these particles have at the location of the satellite are not the same pitch angles they have at the top of the atmosphere. The relation between the pitch angles a particle has at these two points in space is

$$\sin \alpha_{120} = \sqrt{\frac{B_{120}}{B_{850}}} \sin \alpha_{850}$$

where

α_{850} = pitch angle at the TIROS-N spacecraft 850 km

α_{120} = pitch angle at 120 km (the foot of the field line)

B_{850} = geomagnetic field strength at the TIROS-N spacecraft

B_{120} = geomagnetic field strength at the FOFL

Figure 11 illustrates how the pitch angle of a charged particle varies as it moves along the geomagnetic field line between TIROS-N and the atmosphere. Note that convention defines a particle's pitch angle as the angle between the particle's velocity vector and the direction of the magnetic field. This means that in the northern hemisphere charged particles moving downwards toward the atmosphere have pitch angles between 0° and 90°. In the southern hemisphere charged particles moving towards the atmosphere have pitch angles between 180° and 90°.

Note also that it is possible for $\sin \alpha_{120}$ to exceed 1.0 such that $\sin \alpha_{120}$ is not defined. Physically, this occurs when the charged particles going downwards toward the atmosphere at TIROS-N in fact magnetically mirror before reaching 120 km and return back up the magnetic field line. Such particles cannot be counted as contributing to the energy influx into the earth's atmosphere.

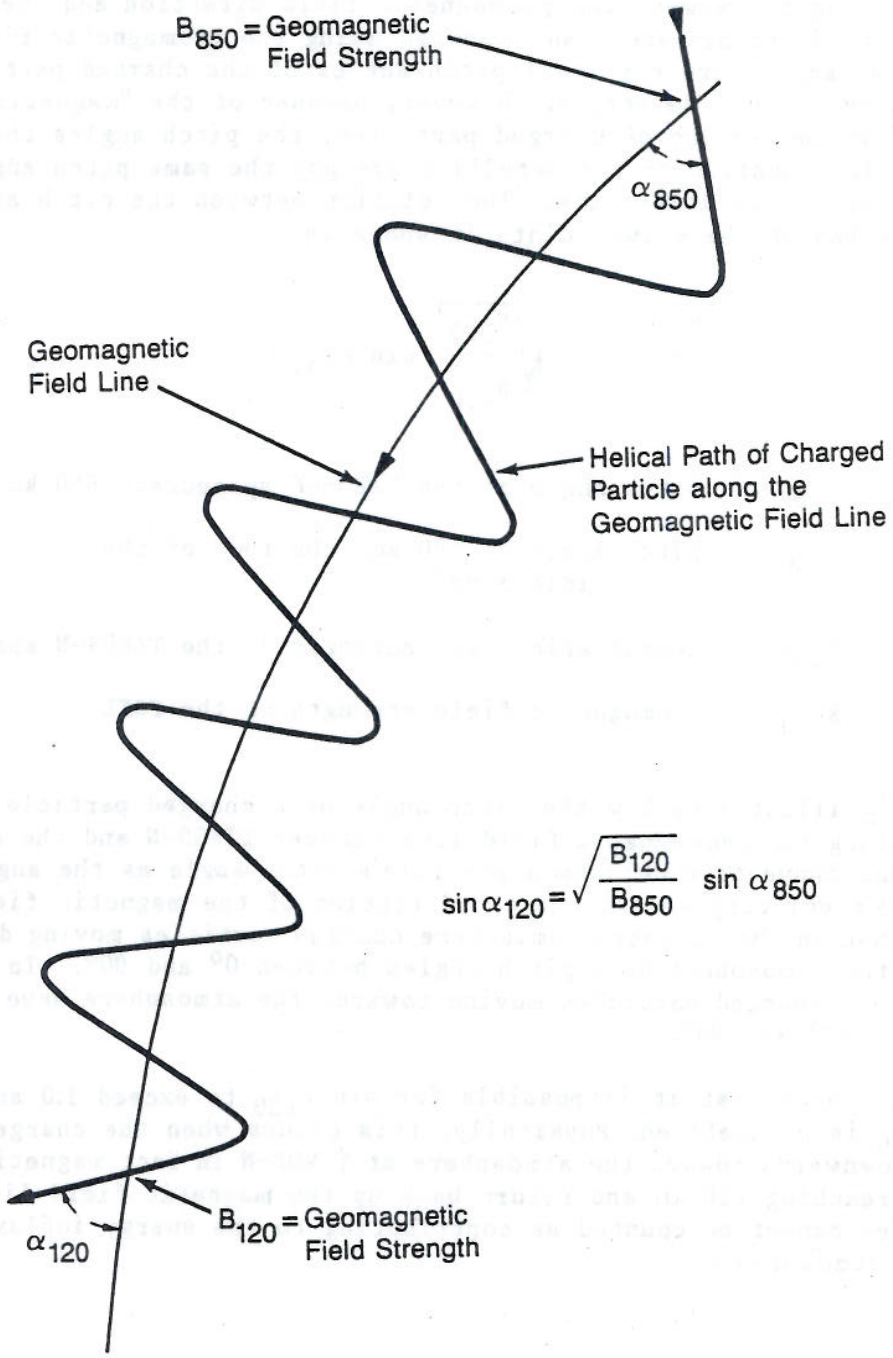

Figure 11.—Variation of Particle Pitch Angle Along Field Line

Using the measurements of 0EFD, 30EFD, 0PFD, and 30PFD, together with the pitch angles at which the measurements were made (as transformed to 120 km) F_T, the integral shown on p. 14, may be evaluated independently for both electrons and ions. The sum of these two, converted to physical units erg/(cm^2·s), becomes the Total Energy Flux.

During the creation of the archive tapes at SEL, all variables concerning the geomagnetic field are computed once each eight seconds and given in the header format. Amongst these variables are:

A. The three vector components of the geomagnetic field at TIROS-N together with the scaler magnitude of the field.

B. The geographic coordinates of the FOFL.

C. The geomagnetic coordinates of the FOFL.

D. Local solar time and geomagnetic time of the FOFL.

E. The three vector components of the geomagnetic field at the FOFL together with the scaler magnitude of the field.

F. The pitch angles of the charged particles being observed by the two TED detectors as transformed to the FOFL.

If neither of the two detectors is viewing charged particles which reach the earth's atmosphere, then the value of the total energy is set to 0 on the archive tape. However, the values of 0EFD, 30EFD, 0PFD, and 30PFD remain available in the record. The situation where neither detector views charged particles which can reach the atmosphere is confined to low geographic latitudes where energy flow into the atmosphere is small.

The TED was originally designed to operate in any one of three different modes in order to compensate for possible detector failures. However, the TED has thus far proven reliable. This fact, coupled with the additional data processing complexity in handling varying instrument modes of operation, led to the policy that the TED is operated only in its normal mode.

As a quality check on the operation of the TED, the counts during the first 1/13 second (background phase) of each sweep are accumulated for 16 sweeps - a total of 1.23 seconds. The accumulated count is transmitted once each 32 seconds in place of the normal transmission of 0DE1, 0DE3, 0DE5, and 0DE7. There are 4 such numbers abBK where a = 0, 30 and b = E, P while BK means background. These numbers are generally less than 50. Should they exceed 200, detector malfunction may have occurred.

When analyzing TED data, take care in treating total energy flux values which exceed 100 ergs/(cm^2·s). Experience has shown that a high percentage of such data (~50%) are in fact associated with telemetry noise and do not represent valid observations.

3.5 TED Application

The TED instrument was included in the TIROS-N SEM to monitor the total energy fluxes carried to the atmosphere by energetic charged particles (energies between 0.3 keV and 20 keV). The purposes for doing so are twofold.

1. To provide a measure in near real time of the general level of particle precipitation activity. In this respect, it should be mentioned that the particles being measured are those that produce auroras. Thus the data provides a direct measure of the intensity and extent of the aurora beneath the track of the satellite and allows estimating the potential effects on radio communications and navigation equipment operating in the auroral zone. Several aspects of the data can be used to generate usable indices of activity. Among these are:

    a. The most equatorward latitude for which the energy flux exceeds a given value. This provides an index of the general level of activity.

    b. The maximum energy influx recorded during a given satellite pass. This is equivalent to a measure of the brightest aurora beneath the satellite.

    c. The latitude and longitude integrated total energy input. This value weights both the intensity and the extent of the energy input, and provides an estimate of global auroral activity.

2. The second purpose of the instrument is to generate a data base useful to the study of the response of the upper atmosphere to the energy input from the magnetosphere. A measure of the energy input to the atmosphere above 100 km is useful (and relevant) for correlation with atmospheric data.

3.6 Data Displays for the TED

TED data may be displayed as a graph of the particle energy influx for a particular orbit, as shown in Figure 12. Such data may be used to estimate the total amount of particle energy being deposited into the entire auroral atmosphere. Figure 13 shows these power input estimates averaged over an entire day (about 29 satellite passes) for an entire month.

It should be pointed out that the power input due to particles is only 30% of the total power input to the atmosphere from magnetospheric processes. The rest comes from Joule heating caused by ionospheric currents driven from the magnetosphere. The total of both power inputs to the upper atmosphere often exceeds the energy input to the same altitude range from solar radiance.

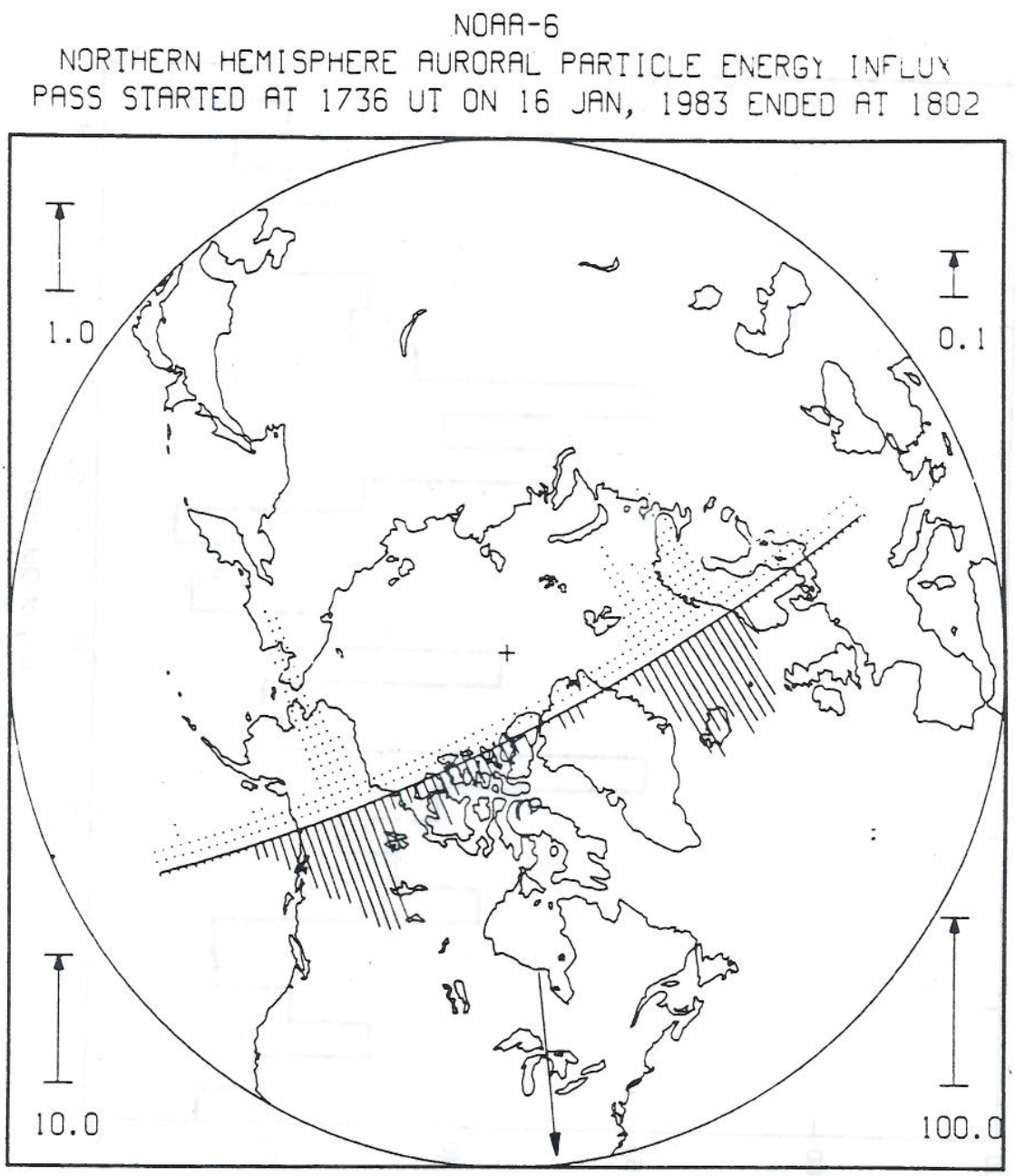
NOAA-6
NORTHERN HEMISPHERE AURORAL PARTICLE ENERGY INFLUX
PASS STARTED AT 1736 UT ON 16 JAN, 1983 ENDED AT 1802
1.0
0.1
10.0
100.0
REFERENCE SCALES ARE IN UNITS OF ERGS/CM2/SEC

Figure 12

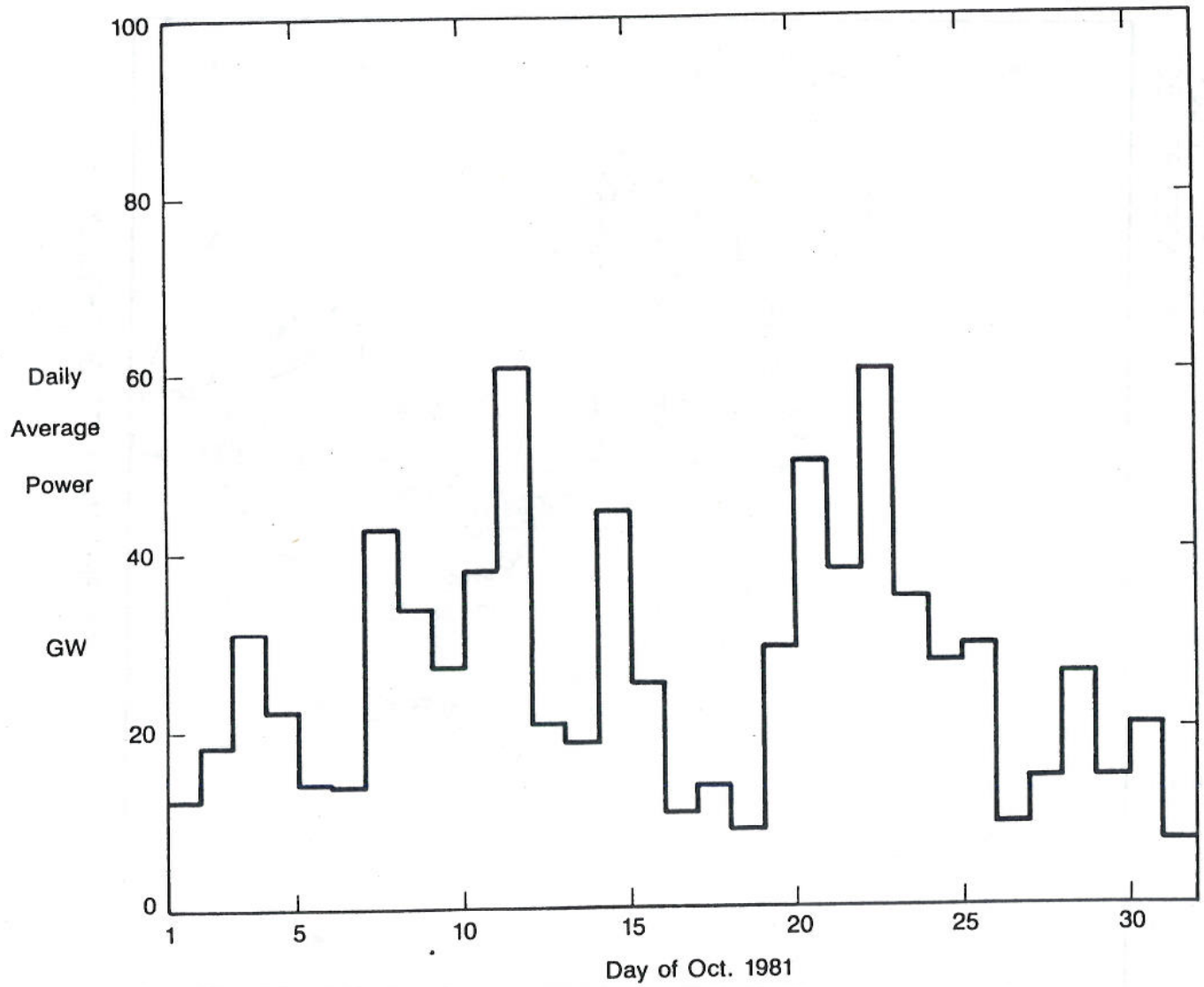

Figure 13.—Hemispherical Power Input

4. MEDIUM ENERGY PROTON AND ELECTRON DETECTOR (MEPED)

4.1 General Description

The MEPED uses solid-state silicon detectors to detect electrons, protons, and alpha particles over an energy range of >30 keV to >80 MeV. The silicon detectors are linear detectors which produce a quantity of charge directly proportional to the quantity of energy deposited in the active volume of the detector by an incident particle. This makes possible the energy analysis of the particle flux by analyzing the distribution of the charge pulses produced by the incident particles. A general view of the instrument is shown in Figure 14. Separate pairs of proton and electron "telescopes" are used, one pointing at approximately 0^{o} to the magnetic field at high latitudes, the second of the pairs nominally perpendicular to the first.

In addition three simple sensors measure omnidirectional fluxes of higher energy protons. These use detectors in a dome moderator arrangement in which the energy threshold is basically defined by the energy loss in the shielding moderators.

A functional block diagram of the MEPED is shown in Figure 15.

Each detector has its own charge sensitive preamplifier. The output of each of the six preamps associated with the 0^{o} and 90^{o} telescopes are multiplexed into three signal chains consisting of linear amplifiers and pulse shaping networks which drive a set of pulse amplitude discriminators. The three high energy integral channels have individual, separate signal chains with only a single discriminator. These discriminators, either directly or in logical combination or in the case of the proton telescopes, after time coincidence gating and logical combination, produce logic level pulses for transmission to the DPU which correspond to the intensity of a given incident particle species in particular energy bands.

It is of interest to note that at the lowest threshold of this sensor, 30 keV, the linear signal electronics is detecting an event producing only 10^{4} electrons at the input to the charge sensitive preamplifier.

The MEPED telescopes consist of four sensors, a pair of which view the local zenith and a pair of which "look" ~90^{o} to this direction. Each pair of sensors consists of a proton telescope and an electron telescope. The zenith is the spacecraft -X axis as shown in Figure 3 and +Y is the direction of spacecraft velocity. The 90^{o} sensors "look" nominally along the -Z axis. In order that the viewing cone of these sensors be unobstructed by a sunshade the collimator axes were rotated (around the Y axis) away from -Z toward -X by 7^{o} and 9^{o} for the electron and proton detectors respectively.

4.2 Proton Telescope

Each proton telescope responds to protons (actually to all positive ions) with energy >30 keV in five discrete energy intervals. Low energy electrons are removed by a broom magnet. Higher energy electrons and ions are discriminated against by anticoincidence logic between the two solid state detectors in the telescope. The proton telescope also identifies the intensity of ions with $Z \geq 2$ in one energy interval.

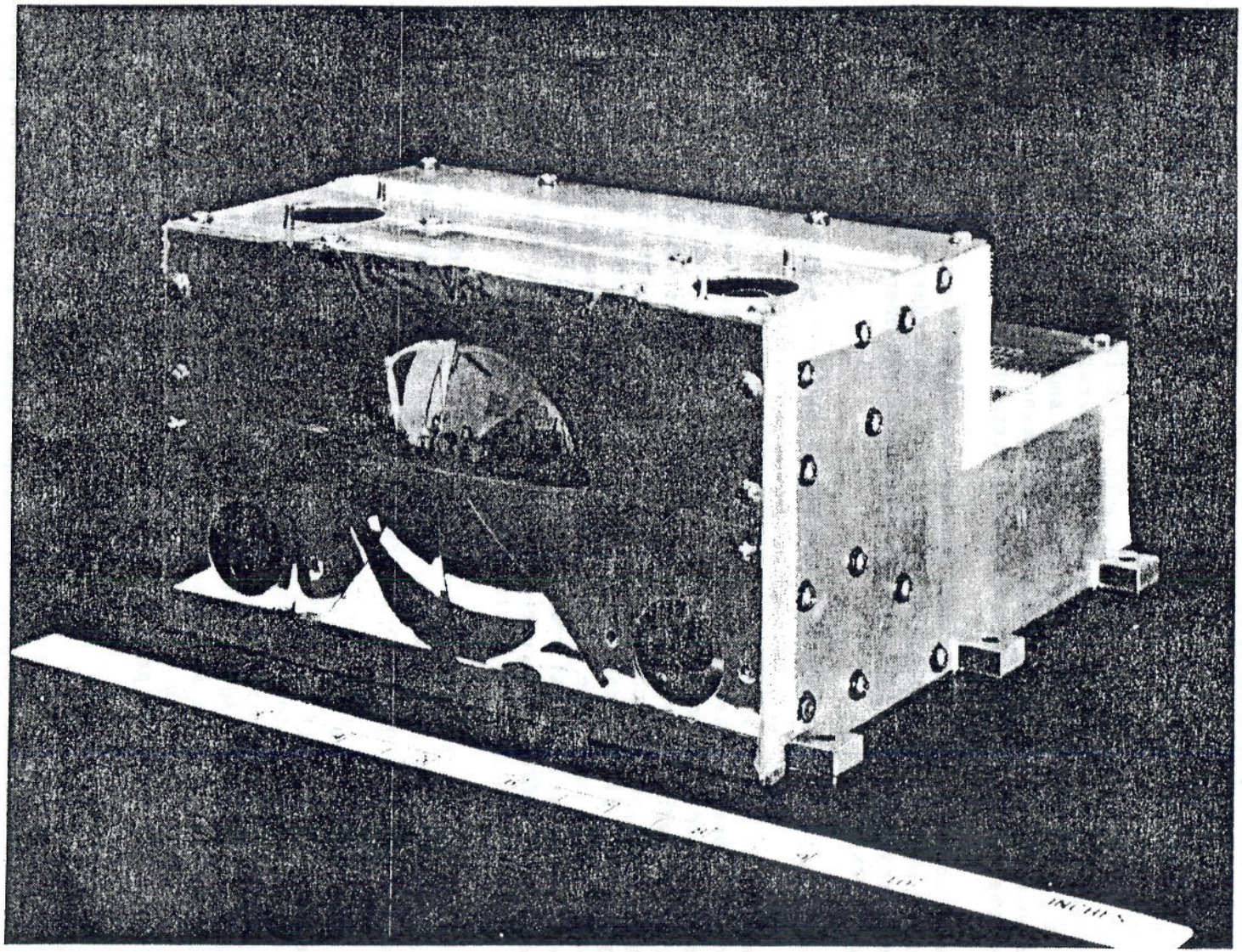

Figure 14.—Medium Energy Proton and Electron Detector

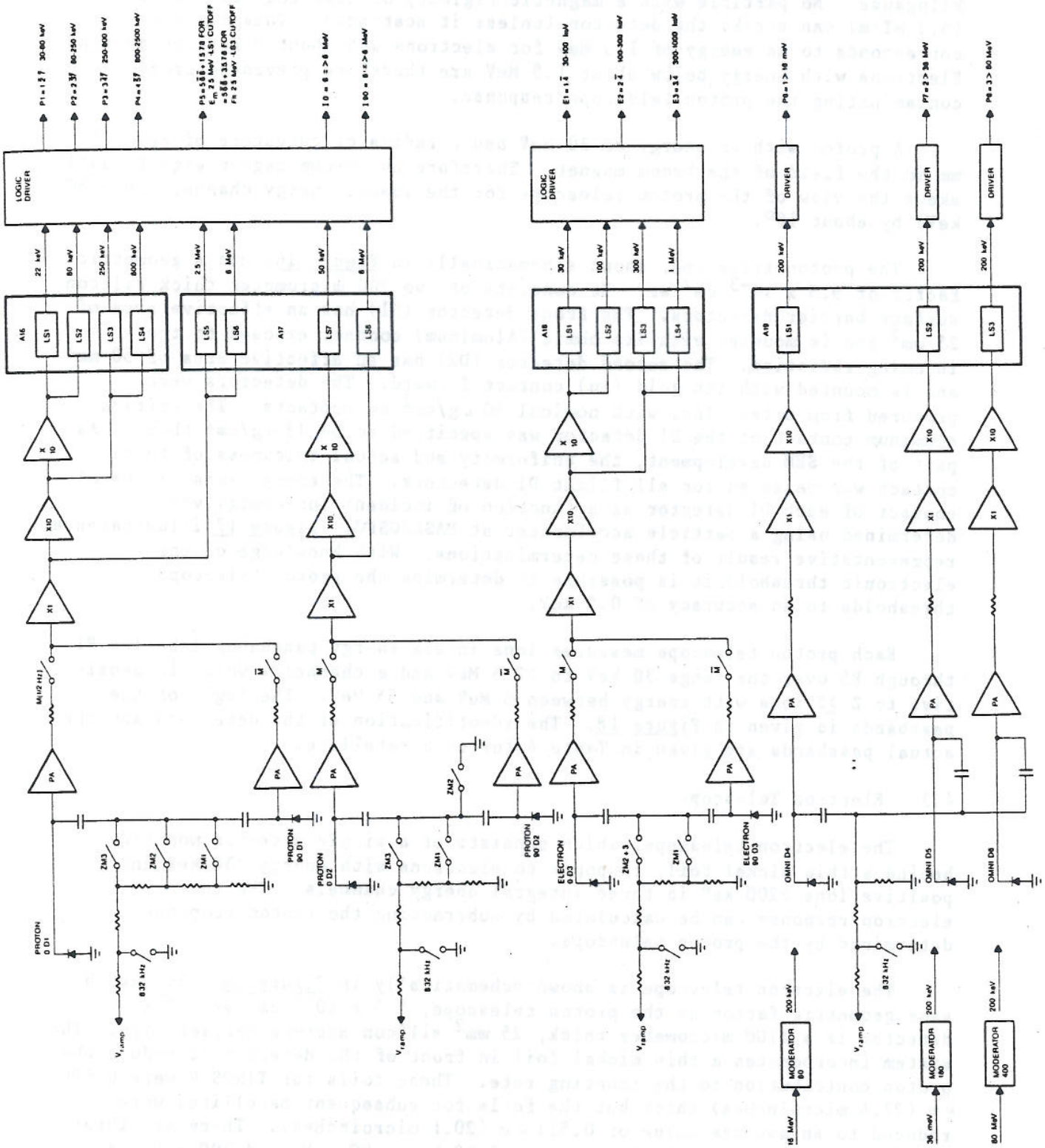

Figure 15.—MEPED Block Diagram

The broom magnet, made of Alnico VIII, has a strength of at least 2.48 kilogauss. No particle with a magnetic rigidity of less than 6200 gauss-cm (6.2 mT·m) can strike the detector (unless it scatters). This rigidity corresponds to an energy of 1.5 MeV for electrons and about 2 keV for protons. Electrons with energy below about 1.5 MeV are therefore prevented from contaminating the proton telescope response.

A proton with an energy of 30 keV has a radius of curvature of about 100 mm in the field of the broom magnet. Therefore the broom magnet significantly skews the view of the proton telescope for the lowest energy channel (30 - 80 keV) by about 10°.

The proton telescope, shown schematically in Figure 16, has a geometric factor of 9.5×10^{-3} cm^2·sr. It consists of two 200 micrometer thick silicon surface barrier detectors. The front detector (D1) has an effective area of 25 mm^2 and is mounted with its ohmic (Aluminum) contact exposed to the incoming radiation. The second detector (D2) has an effective area of 50 mm^2 and is mounted with its gold (Au) contact forward. The detectors were procured from Ortec, Inc. with nominal 40 μg/cm^2 Au contacts. The critical aluminum contact of the D1 detector was specified to be 18 μg/cm^2 thick. As part of the SEM development, the uniformity and actual thickness of this contact was measured for all flight D1 detectors. The energy loss in the Al contact of each D1 detector as a function of incident ion energy was determined using a particle accelerator at NASA/GSFC. Figure 17 illustrates a representative result of these determinations. With knowledge of the electronic threshold it is possible to determine the proton telescope thresholds to an accuracy of 0.5 keV.

Each proton telescope measures ions in six energy passbands labelled P1 through P5 over the range 30 keV to >2.5 MeV and a channel I which is sensitive to Z $\geq$2 ions with energy between 6 MeV and 55 MeV. The logic of the passbands is given in Figure 18. The identification of the detectors and the actual passbands are given in Table 4 for each satellite.

4.3 Electron Telescope

The electron telescope, which consists of a single detector mounted behind a thin nickel foil, responds to electrons with energy >30 keV and positive ions >200 keV in three integral energy channels. The true electron response can be calculated by subtracting the proton response determined by the proton telescope.

The electron telescope is shown schematically in Figure 19. It has the same geometric factor as the proton telescope, 9.5×10^{-3} cm^2·sr. The detector is a 1700 micrometer thick, 25 mm^2 silicon surface barrier type. The system incorporates a thin nickel foil in front of the detector to reduce the proton contribution to the counting rate. These foils for TIROS-N were 0.696 μm (27.4 microinches) thick but the foils for subsequent satellites were reduced to an average value of 0.511 μm (20.1 microinches). There are three energy thresholds at nominal energies of 30 keV, 100 keV, and 300 keV. A fourth threshold was included at approximately 1 MeV, used as a veto signal to

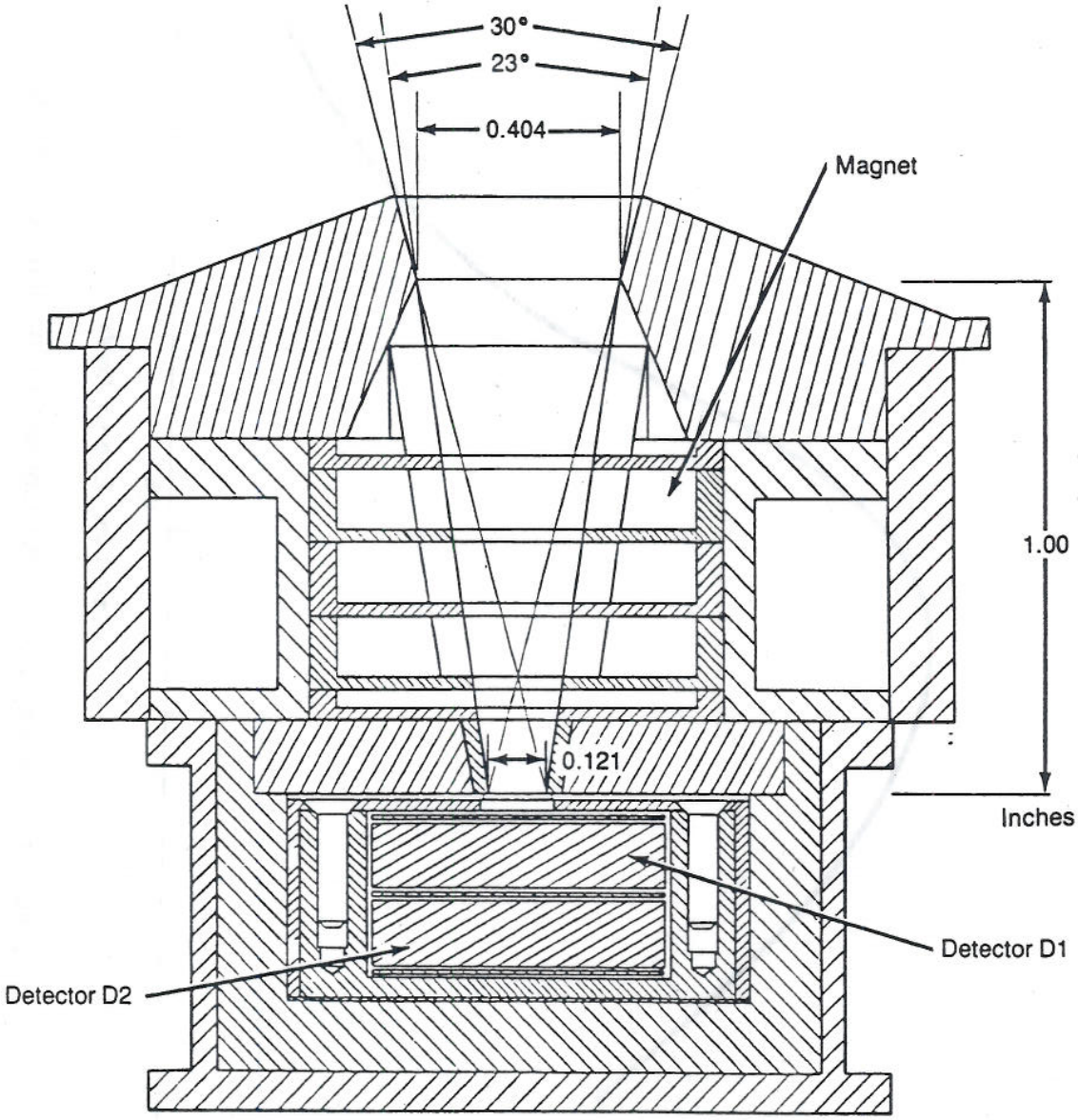

Figure 16.—MEPED Proton

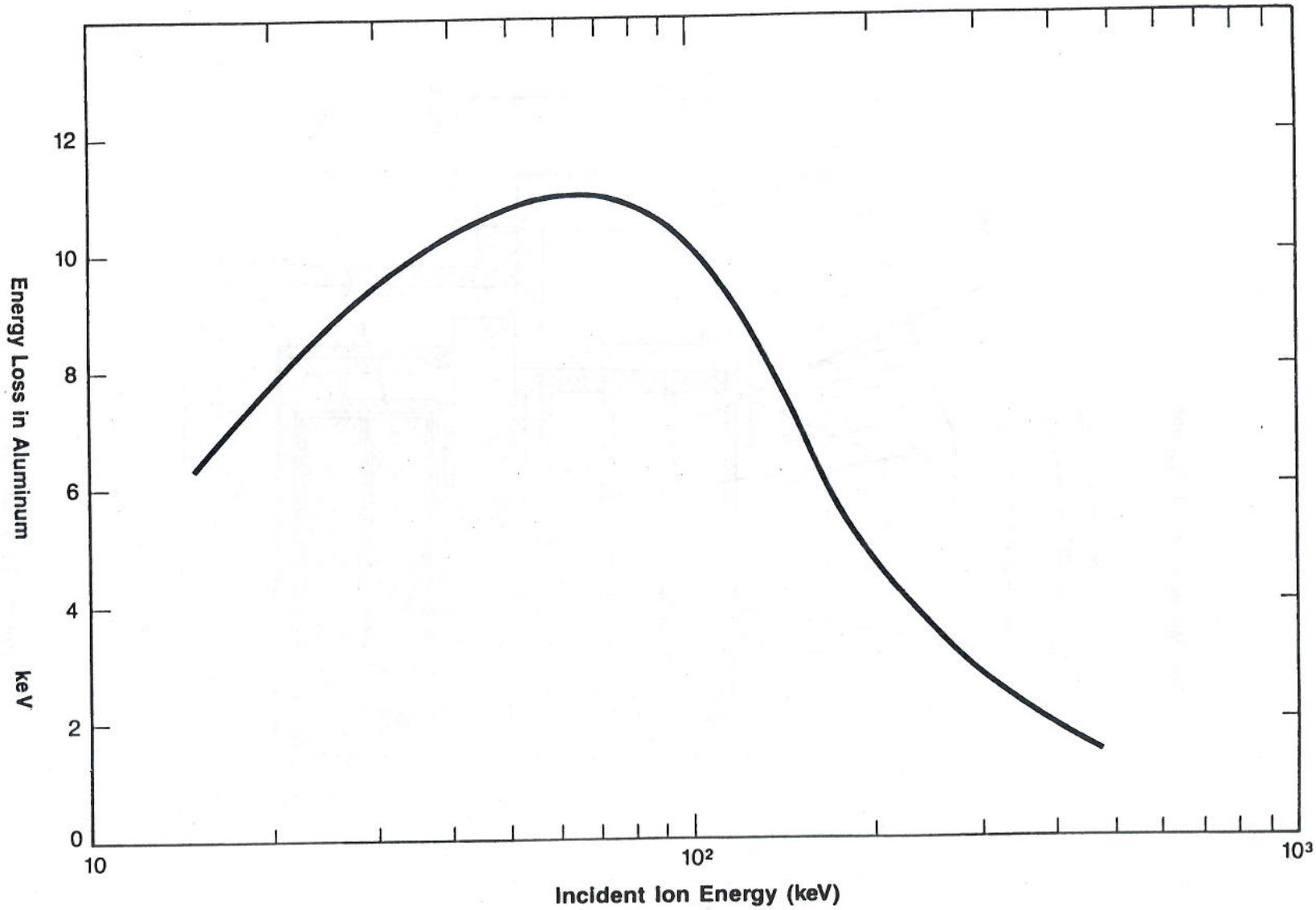

Figure 17.—Energy Loss in A1 Contact *vs* Incident Ion Energy

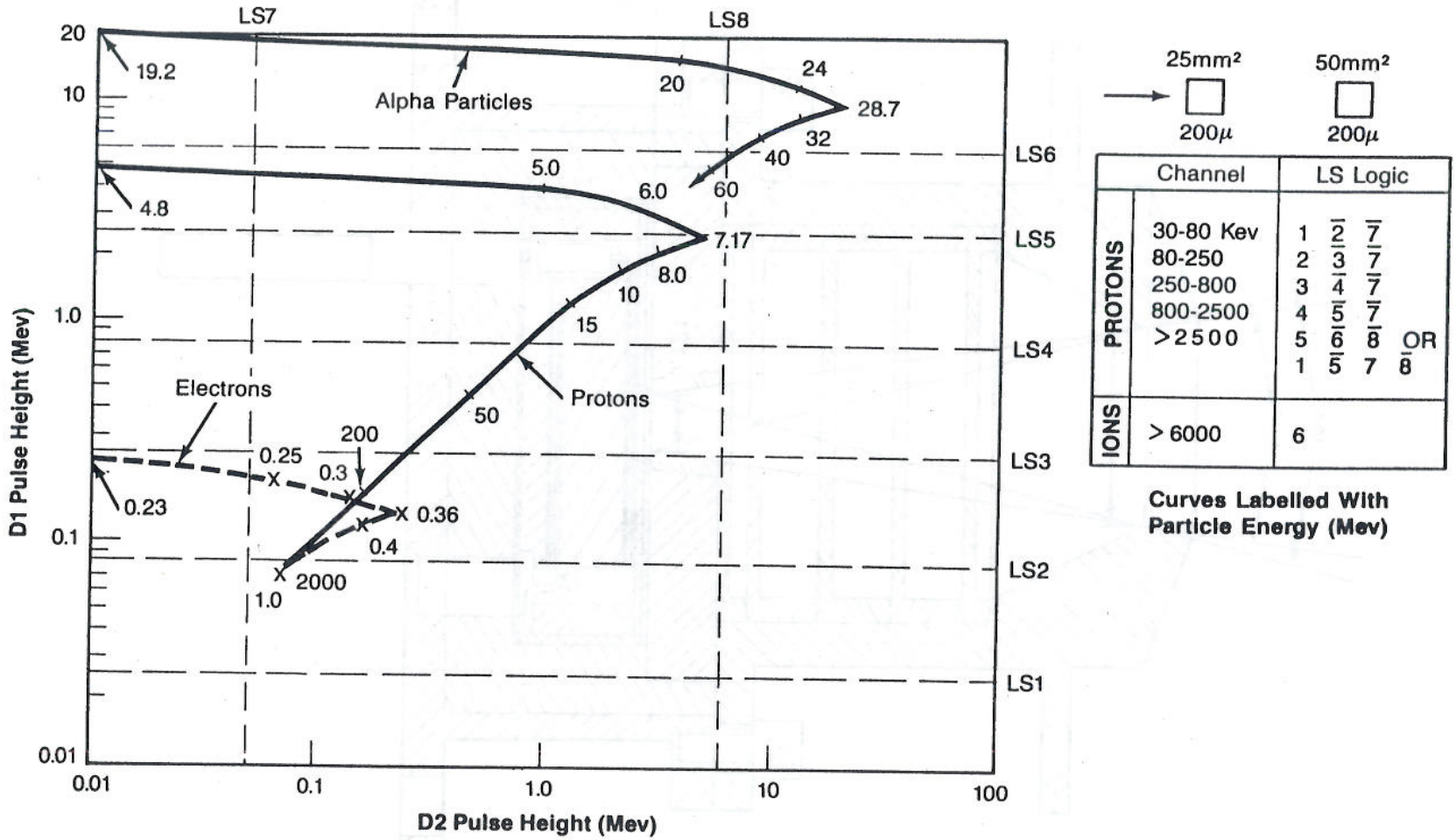

Figure 18.—MEPED Proton Telescope Response

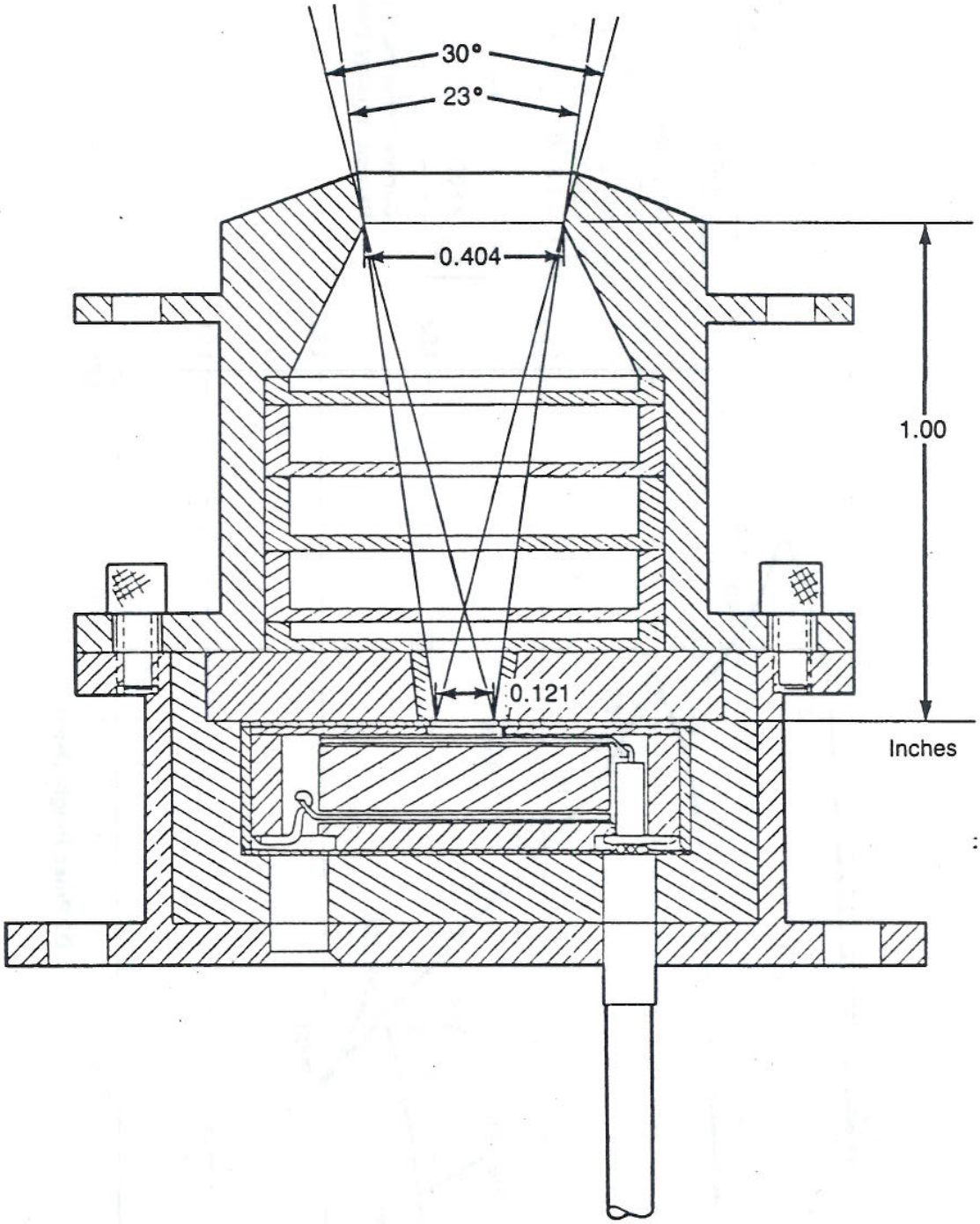

Figure 19.—MEPED Electron Telescope

effectively remove any sensitivity to protons above 1.1 MeV. Figure 20 presents the nominal pulse height response of the electron detector.

The actual thresholds for TIROS-N (0.696 μm (27.4 microinch) Ni foil) were determined from electron beam calibrations, presented in Figure 21, using the accelerator facilities at NASA/GSFC. No detailed calibrations were performed on the subsequent satellite assemblies. The electron incident energy thresholds have been estimated by simply adding 5 keV to the electronic thresholds for the subsequent units. The actual thickness of the Ni-foils for NOAA-A and -B are not known but a nominal or average value for all foils was used to make the estimate. These thresholds are given in Table 3 along with the range of proton energies to which that channel is sensitive (enclosed in brackets).

TABLE 3. MEPED Detector Data and Passbands

TIROS-N Protoflight Model					
D1	17-294E	17-294I	D3	17-097B	17-098D
D2	17-107E	17-108I	foil	27.4 microinch Ni	
P1	41.7-82.9keV	39.6-79.6 keV	E1(e)	>40 keV	>40 keV
P2	82.9-265	79.6-254	E1(p)	(177-1128)	(176-1119)
P3	265-860	254-820	E2	>107(262-1128)	>105(260-1119)
P4	860-2784	820-2655	E3	>322(453-1128)	>318(450-1119)
P5	>2.78 MeV	>2.66 MeV	I	6.32-(55) MeV	6.01-(55)MeV
NOAA-A Flight Model 2					
D1	17-102I	17-103E	D3	17-099C	17-098G
D2	17-108D	17-107F	foil ave	20.07 microinch Ni	
P1	30.6-82.6 keV	30.3-80.4 keV	E1(e)	>29	>29.2
P2	82.6-247	80.4-242	E1(p)	(135-1320)	(135-1320)
P3	247-853	242-834	E2	>117(230-1320)	>117(230-1320)
P4	853-2636	834-2579	E3	>350(445-1320)	>350(445-1320)
P5	>2.64 MeV	>2.58 MeV	I	6.94-(55) MeV	6.79-(55) MeV
NOAA-B Flight Model 1					
D1	17-103E	17-101G	D3	17-099F	17-717B
D2	12-122C	17-108A	foil ave	20.07 microinch Ni	
P1	32.9-83.7keV	32.5-81.6 keV	E1(e)	>28 keV	>28
P2	83.7-252	81.6-247	E1(p)	(135-1050)	(135-1040)
P3	252-813	247-801	E2	>105(220-1050)	>104(220-1040)
P4	813-2681	801-2649	E3	>317(415-1050)	>313(410-1040)
P5	>2.68 MeV	>2.65 MeV	I	6.08-(55) MeV	6.0-(55) MeV

D1,D2,D3 refer to the detectors. Serial numbers are listed.
P1, etc. refer to the output data channels from these detectors.

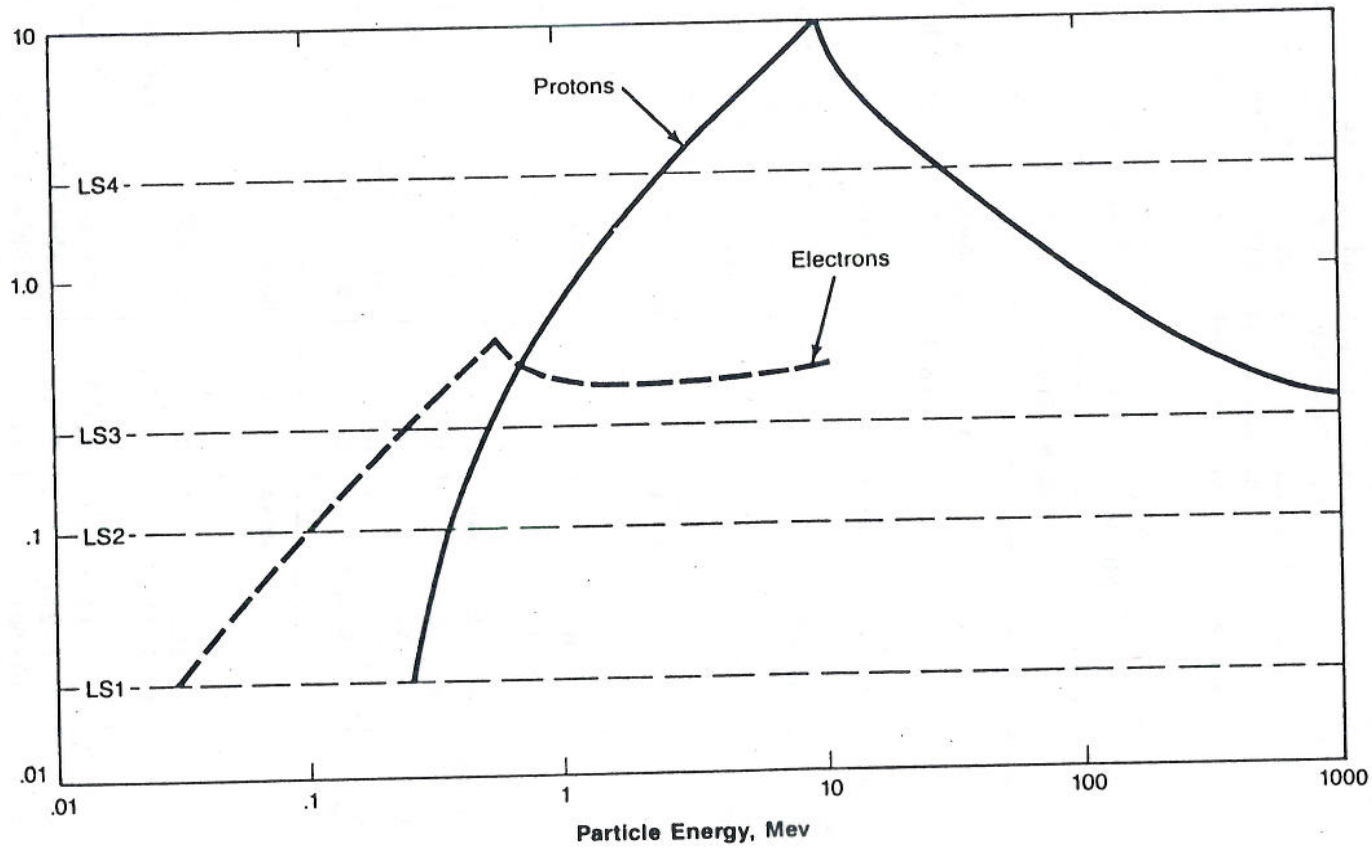

Figure 20.—MEPED Electron Detector Nominal Pulse Height Response

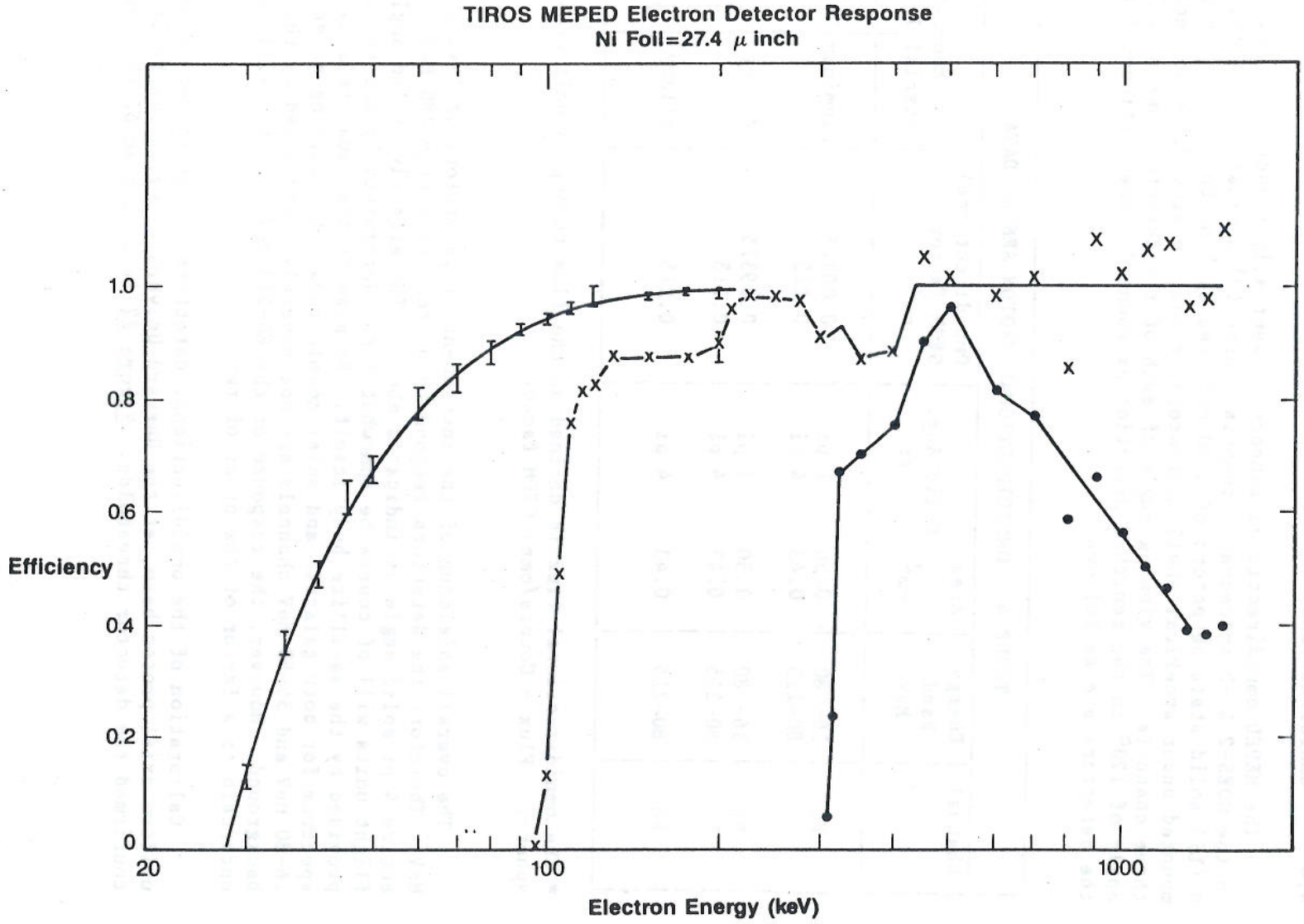

Figure 21.—MEPED Electron Detector Efficiency

4.4 Omnidirectional Sensors

The MEPED omnidirectional sensors, essentially identical to units flown on the GOES-2 & -3 spacecraft, comprise three (3) nominally identical Kevex Si(Li) solid state detectors of 0.50 cm^2 area by 3 mm thickness, independently mounted under spherical shell moderators, domes, to provide measurements in three channels. The viewing angle of each of the detectors has a full opening angle of 120° in the zenithal direction as mounted. The pertinent data for the detectors are as follows:

TABLE 4. OMNIDIRECTIONAL PROTON SENSOR DATA

Channel	Energy Band MeV	Area cm^2	Solid Ang. sr	Omnidirectional GEOM Factor * cm^2	Moderator Material	Moderator Thickness
P6	16- 80	0.50	1 pi	0.09375	Aluminum	.050 in. 1.27 mm
	80-215	0.43	4 pi	0.215		
P7	36- 80	0.50	1 pi	0.09375	Copper	.230 in. 5.84 mm
	80-215	0.43	4 pi	0.215		
P8	80-215	0.43	4 pi	0.215	Mallory	.086 in. 2.18 mm

* The omnidirectional flux is defined as the flux through a unit cross section sphere; Flux = Counts/omni GEOM factor.

The overall shielding of the instrument stops protons of less than 80 MeV. Therefore the detectors respond to protons of energy >80 MeV over the entire 4 pi solid angle as indicated above. The effective solid angle of the flight units will of course be somewhat less, determined by the shielding provided by the satellite body itself. Because of the usual relatively steep spectrum for both galactic and solar cosmic rays, the counting rates of the 16-80 MeV and 36-80 MeV channels are not severely compromised by the >80 MeV background. However, the response of the 80-215 MeV detector will be uncertain to a factor of the order of two.

Calibration of the omnidirectional detectors was performed using a uniform axial proton beam, at the Harvard University Cyclotron Facility, which confirmed the detector thresholds. Figure 22 is a diagram of the detector.

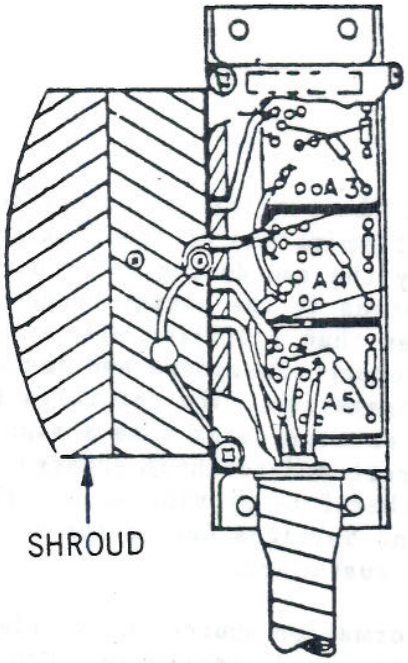

SIDE VIEWS

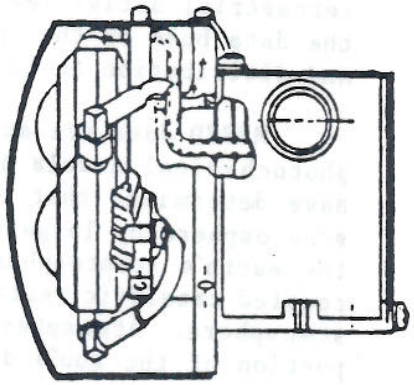

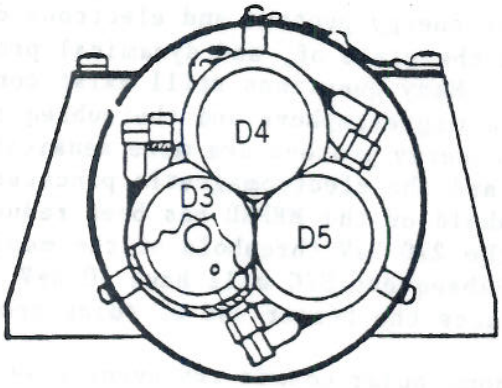

"KEVEX"
Si (Li)
DETECTOR 3 PLACES

D3 = ALUMINUM DOME
D4 = COPPER DOME
D5 = TUNGSTEN DOME

DOME DETECTORS

Figure 22.—Omnidirectional Spectrometer

4.5 MEPED Application

The principal operational use of the particle detectors comprising the MEPED is the reliable and accurate determination of the flux and spectrum of energetic particle fluxes produced by the sun during solar disturbance events. These energetic particles, mostly protons in the energy range of some tens of kilovolts to, in major events, greater than a billion electron volts, produce additional ionization of the Earth's upper atmosphere and ionosphere which has substantial consequences on radio propagation. The particles themselves and their atmospheric secondaries may in extreme cases pose a significant radiation hazard to high flying aircraft and to those engaged in extra-terrestrial activities. These data therefore provide an important input to the data base of the Space Environment Services Center for real time analysis and distribution to their interested customers.

MEPED data are an important information source for validation of photochemical models of the stratosphere and ionosphere. Crutzen et al, 1975, have determined that the additional production of nitric oxide (NO) in the stratosphere by large solar proton events produces substantial reductions in the earth's stratospheric ozone concentration. Nitric oxide, through several coupled catalytic reactions, is efficient in removing ozone from the atmosphere. Atmospheric ozone is important in screening us from a large portion of the sun's damaging ultraviolet radiation.

Additionally, however, the lower energy protons and electrons detected by the MEPED can provide information on the state of, and dynamical processes occurring within, the magnetosphere. Many questions still exist concerning the entry of solar particles into the magnetosphere and the subsequent processes which act upon them. Low energy protons are more sensitive to the properties of the geomagnetic field and the electromagnetic processes they are subject to. The lowest energy threshold of the MEPED has been reduced to 42 keV (in NOAA-A) in channel P1 from the 270 keV threshold of the monitors aboard the previous TIROS series. Subsequent S/C will have 30 keV. This reduction of minimum threshold enhances the tracer use of solar protons.

In the early part of at least some solar cosmic ray events, an asymmetry has been observed between the fluxes seen over the northern and southern polar caps. In comparison with corresponding measurement of the particle fluxes outside the magnetosphere, this asymmetry supports the hypothesis that the interplanetary magnetic field is interconnected with the polar field of the earth. The sense of the connection depends on the direction of the interplanetary field, whether toward or away from the sun. In this manner, observation of solar protons over the polar caps says something about the topology of the geomagnetic fields at high latitudes as well as about the mean orientation of the interplanetary field. Further, solar protons of a given energy have essentially free access to the polar caps of the Earth to some minimum geomagnetic latitude which is dependent upon energy, the so-called cutoff latitude. The cutoff latitude for a given energy is dependent on the local time, an expression of the longitudinal asymmetry of the magnetospheric fields, and is dependent as well on the geomagnetic disturbance level of the magnetospheric fields. A better understanding of the behavior of solar

protons will help define the dynamical changes in the topology of the magnetic field of the earth.

Figure 23 shows data from a portion of one revolution of NOAA-8 in which the satellite went through the auroral zone. The base lines (where log count = 0) are each offset by 10. Longer-term observations are shown in Sauer 1984.

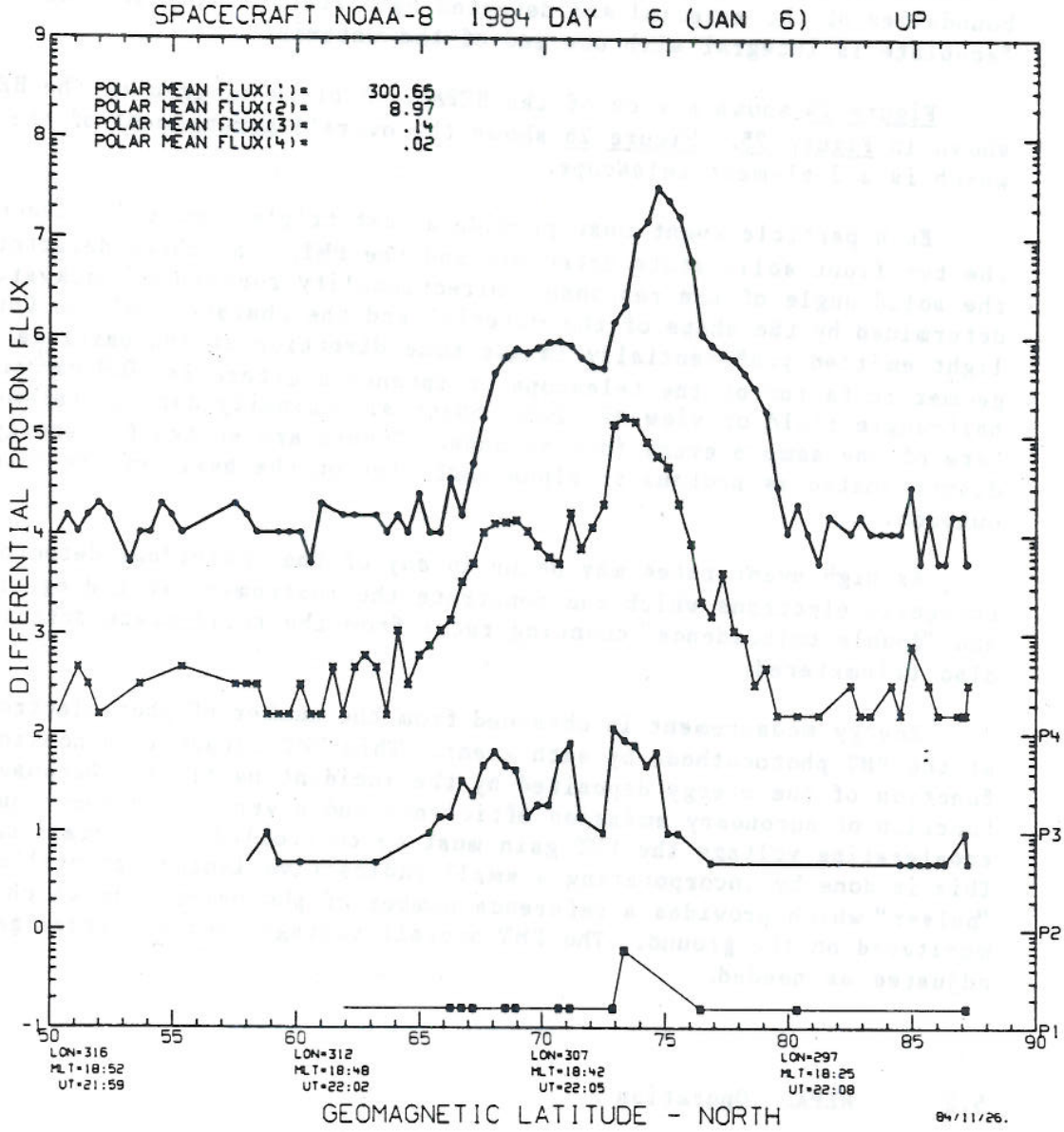

Figure 23.—MEPED Data

5. HIGH ENERGY PROTON AND ALPHA DETECTOR (HEPAD)

5.1 General Description

The HEPAD uses Cerenkov light to detect protons with energy above 370 MeV and alpha particles with energy above 640 MeV. Cerenkov radiation of light occurs when an incident particle travels at greater than the local speed of light in a high-refractive-index material. The material chosen in this case is fused silica. The light is collected by total internal reflection at the boundaries of the material and detected by a Photo Multiplier Tube (PMT) whose faceplate is integral with one end of the material.

Figure 24 shows a view of the HEPAD. A block diagram of the HEPAD is shown in Figure 25. Figure 26 shows the overall arrangement of the sensor which is a 3-element telescope.

Each particle event must provide a fast triple time coincidence between the two front solid-state detectors and the PMT. The three detectors define the solid angle of the response. Directionality forward or backward is determined by the shape of the material and the character of the Cerenkov light emitted preferentially in the same direction as the particle travel. The geometric factor of the telescope acceptance aperture is ~0.9 $cm^2 \cdot sr$ with a half-angle field of view of ~24°. Spectral intensity data is telemetered at a rate of one sample every four seconds. Events are sorted for energy and discriminated as protons or alpha particles on the basis of the detector outputs.

As high event rates may occur in any of the individual detectors due to energetic electrons which can penetrate the instrument shielding, the "single" and "double coincidence" counting rates from the solid-state detectors are also telemetered.

Energy measurement is obtained from the number of photoelectrons produced at the PMT photocathode by each event. This PMT output is a nonlinear function of the energy deposited by the incident particle. Because it is a function of secondary emission efficiency and a very rapid function of accelerating voltage the PMT gain must be controlled to maintain calibration. This is done by incorporating a small radioactive isotope scintillator light "pulser" which provides a reference number of photoelectrons which can be monitored on the ground. The PMT overall voltage, and therefore gain, can be adjusted as needed.

5.2 HEPAD Operation

The HEPAD outputs are listed in Table 5.

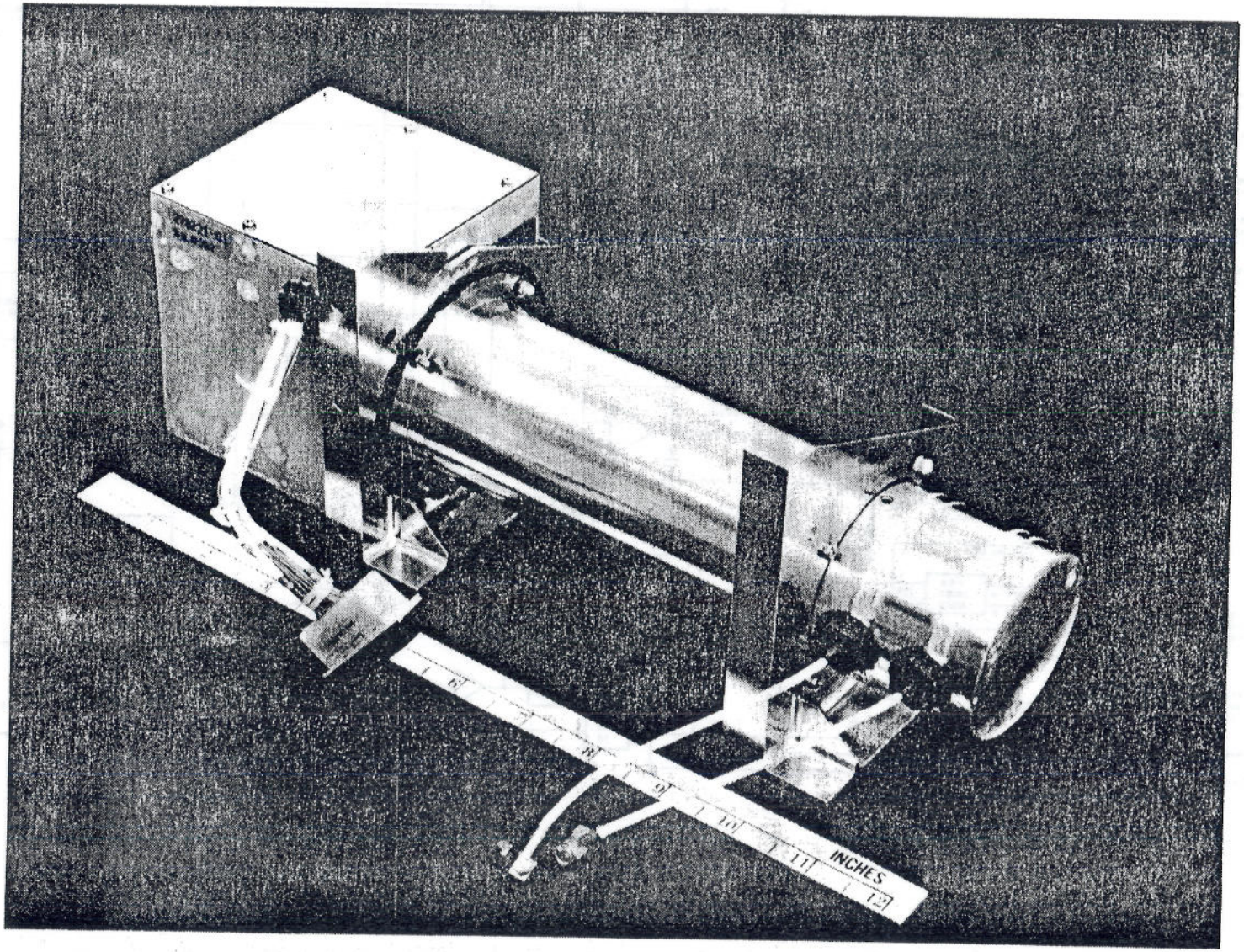

Figure 24.—High Energy Proton and Alpha Detector

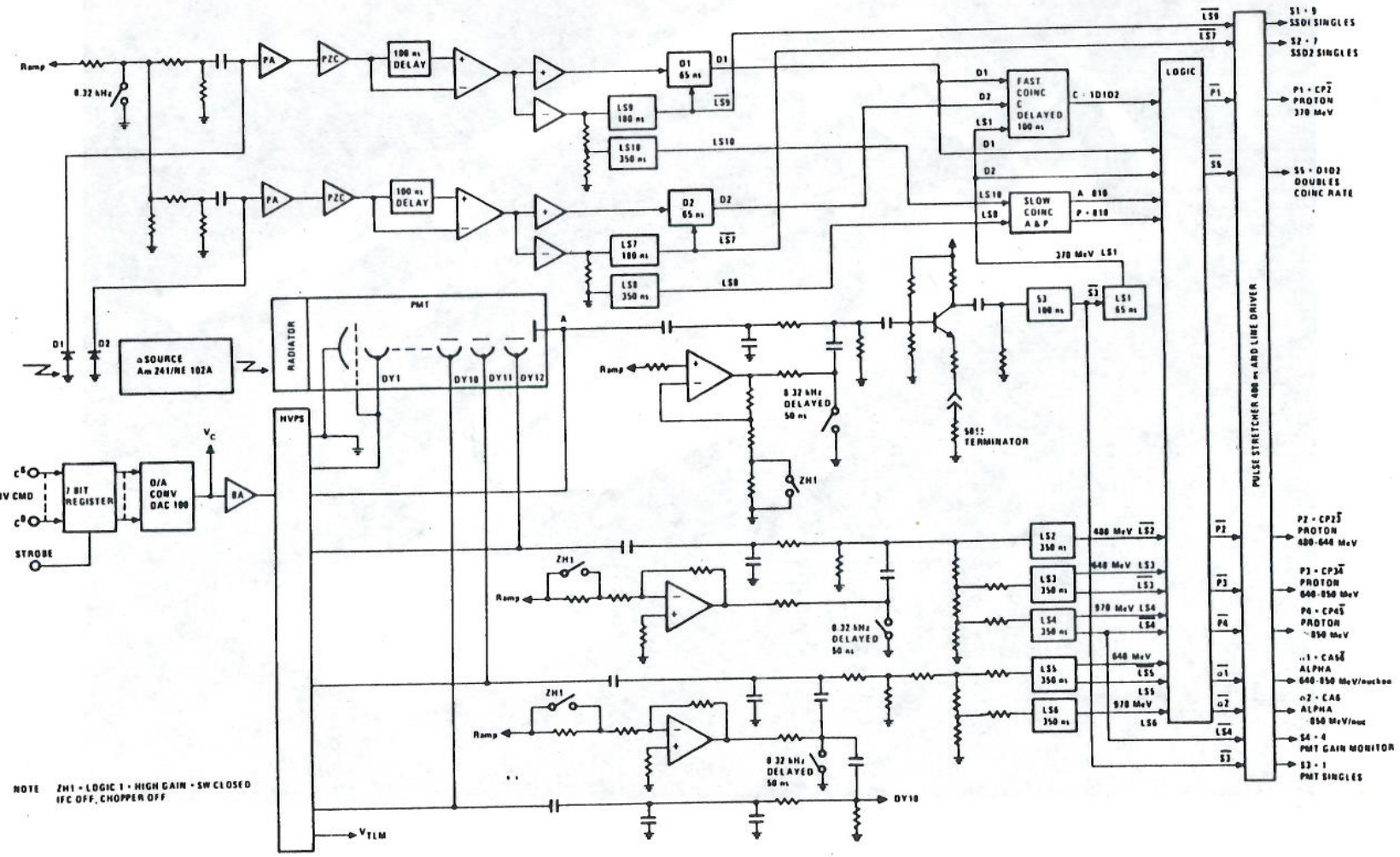

Figure 25.—HEPAD Block Diagram

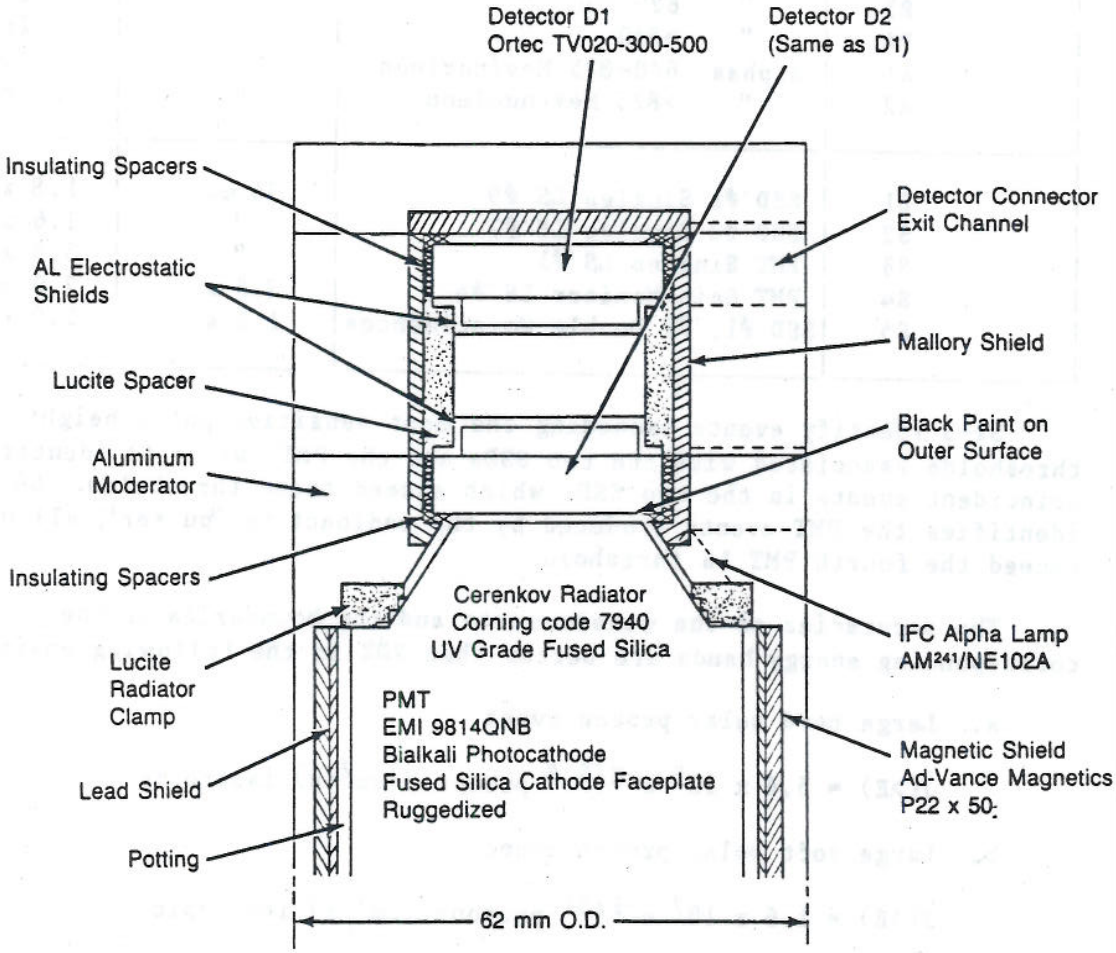

Detector Area: 3 cm^2
Detector Separation: 2.9 cm
Geometric Factor: G ~ 0.9 cm^2-STER
Acceptance Aperture: 68% of G Within $\leq$ 24° Half-Angle
100% of G Within $\leq$ 34° Half-Angle

Figure 26.—HEPAD Telescope Assembly

TABLE 5. HEPAD OUTPUTS

Data Channel	Observable	Count Interval (Nominal)	Nominal Max. Random Rate pps
P1	Protons 370-490 Mev	4 s	620
P2	" 490-620 "	"	420
P3	" 620-850 "	"	260
P4	" >850 "	"	260
A1	Alphas 640-875 Mev/nucleon	"	80
A2	" >875 MeV/nucleon	"	85
S1	SSD #1 Singles LS #9	94 ms	1.8×10^5
S2	SSD #2 Singles LS #7	"	1.6×10^5
S3	PMT Singles LS #1	"	5.6×10^4
S4	PMT Gain Monitor LS #4	2.5 s	2.0×10^3
S5	SSD #1, #2 Double Coincidences	1.2 s	2.0×10^4

S1-3 identify events exceeding the most sensitive pulse height (LS) thresholds associated with the two SSDs and the PMT, while S5 identifies time coincident events in the two SSDs which exceed these thresholds. S4 identifies the PMT events produced by the radioactive "pulser", all of which exceed the fourth PMT LS threshold.

The accuracies of the measurements and the boundaries of the corresponding energy bands are better than 20% in the following environments:

a. Large hard solar proton event

$$J(>E) = 5.4 \times 10^5 \, e^{-E/5.8} \text{ protons}/(\text{cm}^2 \cdot \text{s}) \text{ isotropic}$$

b. Large soft solar proton event

$$J(>E) = 1.6 \times 10^7 \, e^{-P/31} \text{ protons}/(\text{cm}^2 \cdot \text{s}) \text{ isotropic}$$

$$P = (E^2 + 1876E)^{1/2}$$

c. Electron background

$$dJ/dE = 4 \times 10^3 \, E^{-3.3} \text{ electrons}/(\text{cm}^2 \cdot \text{s} \cdot \text{sr} \cdot \text{MeV})$$

where E represents particle energy in MeV.

Figure 26 shows the HEPAD telescope assembly. Two SSD surface barrier silicon detectors D1 and D2 (area 3 cm^2, thickness 500 μm, totally depleted) define an acceptance aperture of ~24° half-angle or geometric factor ~0.9 $\text{cm}^2 \cdot \text{sr}$. All linear trajectories passing through these detectors also pass through the conical fused silica radiator (special PMT faceplate) which has an average thickness of ~17 mm. For an isotropic environment, the probability distribution of path lengths in the conical radiator has a mean value of 1.05 times the average thickness so that the average Cerenkov radiation amplitude

should correspond to traversal of ~18 mm of silica. Silica is employed as the radiator to provide the desired proton energy threshold (~320 MeV) and to allow efficient transmission of the shorter wavelengths of the Cerenkov light (cutoff ~190 nm). Most of the area of the radiator's conical surface is bare to allow total internal reflection of incident Cerenkov light from all trajectories within the acceptance cone. Assuming an average quantum efficiency of 18% and full light collection efficiency within the 200-450 nm interval, 225 photoelectrons should be produced by axial protons of beta ≈ 1 where beta is v/c.

Mallory metal (high-Z) is employed to shield the detectors against bremsstrahlung generated by ambient electrons (thickness is one absorption length for E <350 keV). Similarly, aluminum moderator (low-Z) is employed to shield these detectors against ambient electrons and protons and to suppress the bremsstrahlung radiated by the stopping electrons. Within the out-of aperture solid angle, the moderator will stop protons of <80 MeV and electrons of <7 MeV. For in-aperture directions, the shielding is effective against protons of <65 MeV and electrons of <4 MeV and will absorb ~15 MeV from a 370 MeV proton. Shielding of the detectors from "upward"-entering protons of E <90 MeV is supplied by the silica radiator and the magnetic shield, lead shield, and aluminum shell surrounding the PMT.

The Lucite spacer (see Figure 26) is used to position the detectors in the assembly, while insulating spacers prevent motion of the detector holders in a vibration environment and isolate signal ground (detector shell) from chassis ground. Similarly, the Lucite radiator positions the PMT with respect to the SSD, while contacting only a very small fraction of the radiator area. The aluminum electrostatic shields protect the inner, biased surfaces of the SSDs from EMI capacitively coupled from the structure. To allow monitoring of the PMT quantum efficiency and gain during operation, an Am^{241} radioactive source (5-10 nanocuries) coupled to an NE102A plastic scintillator (thickness 76 μm (0.003"), area 3 x 3 mm) is positioned near the conical wall of the silica radiator to illuminate the entire photocathode with fast light pulses of chosen amplitude (~30% FWHM). The upbeam surface of the silica radiator is blackened to reduce the light collection efficiency for "upward-moving" particle trajectories which intersect D1 and D2.

5.3 Response to Radiation

Figure 27 shows the nominal response of the silicon detectors and PMT to protons and alphas. The abscissa shows the energy lost in each silicon detector, while the ordinate shows either the number of photoelectrons produced in the PMT (solid curves) or the ionization energy loss in silica (dashed curve). The solid line trajectory for protons above 370 MeV is confined within the 125-500 keV abscissa range and the 21-500 photoelectron ordinate range, while the trajectory for alphas above 640 MeV lies above the 500 keV and 500 photoelectron levels. The data handling circuit associated with the telescope contains ten pulse height discriminators (level sensors = LS) at the abscissa and ordinate levels shown in Figure 27, so that protons are distinguished from alphas on the basis of LS8 and 10 (silicon detectors) and LS5 (PMT). Energy analysis of each particle type is provided by the PMT LS1-6, while out-of-aperture events are suppressed by requiring a fast triple coincidence between LS1, 7, and 9 for any event to be counted.

The table on Figure 27 shows the energy ranges of the data channels

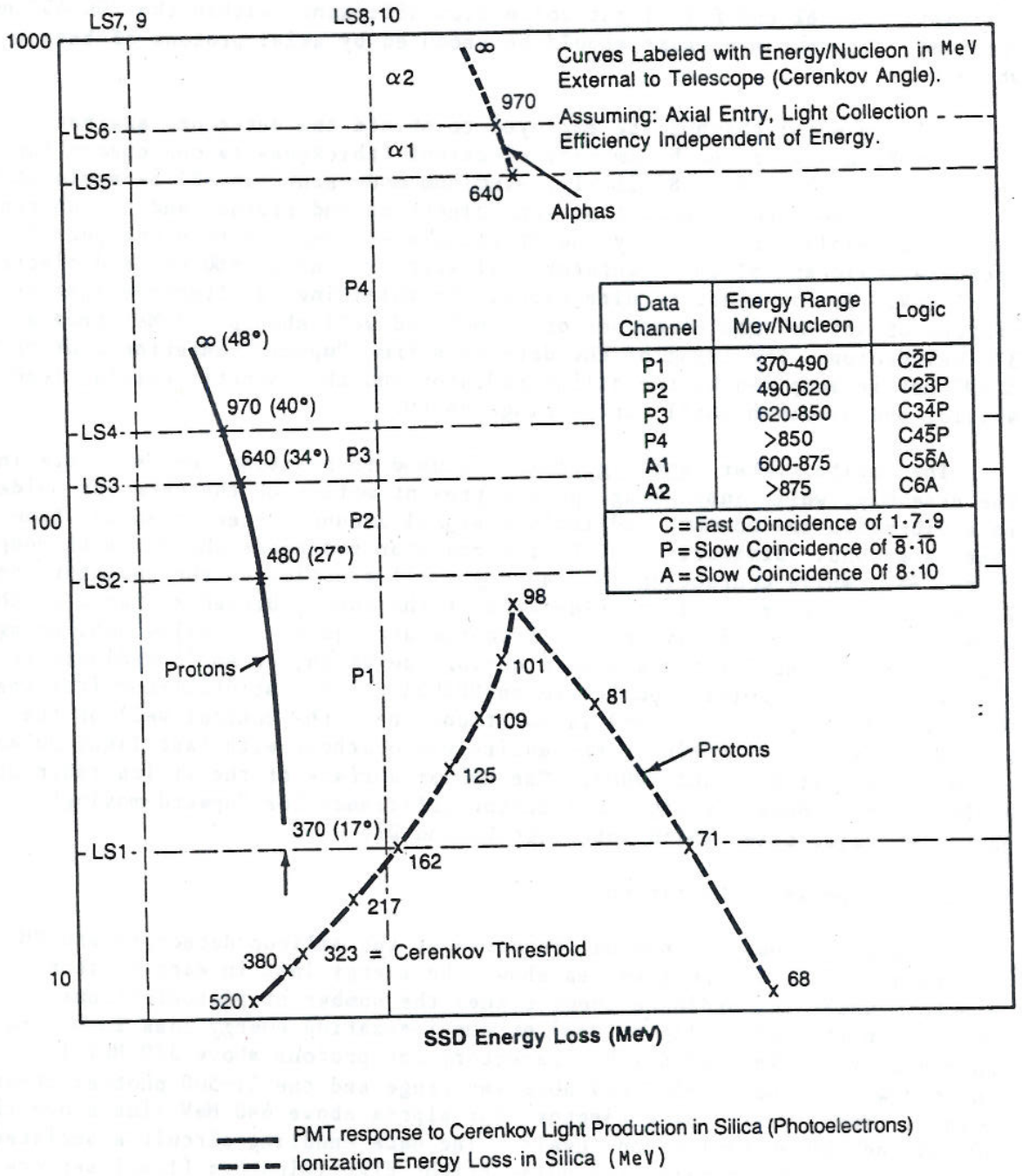

Figure 27..—HEPAD Telescope Response

provided by the HEPAD and the coincidence logic employed to obtain these signals. The dashed line indicates the energy dependence of scintillation produced in the radiator. This curve is not normalized with respect to the Cerenkov trajectories, since the normalization depends on the scintillation efficiency of the silica. This efficiency is sufficiently small that no distortion of the energy dependence of the Cerenkov light is produced by scintillation.

The detector thickness of 500 μm is a compromise between lower cost with lower bremsstrahlung sensitivity (smaller thickness) and greater S/N ratio (greater thickness). The radiator thickness is chosen sufficiently large so as to produce a PMT pulse of >100 photo-electrons for 850 MeV protons, restricting the statistical fluctuation in height of this pulse to about 10% corresponding to a resolution of 170 MeV at 850 MeV. The center of the Am^{241} pulse height peak falls near LS4. The LS4 counting rate (~50 pps) is related to the overall PMT transfer function (silica transmission, PMT quantum efficiency, PMT gain) such that changes can be observed during quiescent periods.

5.4 HEPAD Application

The HEPAD senses the intensity in the local zenith direction of ambient solar and galactic protons above 370 MeV in four energy bands and of ambient solar and galactic alpha particles above 640 MeV in two energy bands.

The occurrence of large solar events with measurable proton flux in the energy range covered by the HEPAD is very infrequent. While infrequent, the occurrence of solar cosmic ray events with significant fluxes of particles above several hundred MeV is important for both scientific and operational reasons. Protons at the top of the atmosphere with energies greater than 60 MeV can penetrate to aircraft altitudes (24 km, 80,000 ft.) and with greater than about 650 MeV can penetrate the entire atmosphere and reach the earth's surface producing so-called ground level events. These very energetic events produce low altitude ionospheric effects, and may also constitute a radiation hazard at aircraft altitudes.

The last HEPAD on the NOAA Polar Orbiting satellites was flown on NOAA-7 launched on 6-23-81. The remaining four HEPADS were transferred to the GOES program for flight on GOES D, E, F and G.

5.5 Sample of HEPAD Data

Kolasinski has compared the inner zone spectrum measured by the HEPAD on TIROS with the AP-7 model published by Lavine and Vette. For L = 1.20, they give a characteristic flux J_o of 644 protons/($cm^2 \cdot s \cdot sr$) for J perpendicular to the field at B = 0.18 gauss and an e-folding energy of E_o = 160 MeV. (L is the maximum radius of a field line given in earth radii). Similarly at B = 0.19, they give J_o = 422 and E_o = 140 MeV. The HEPAD spectrum gives E_o = 145 MeV and J = 800 protons/($cm^2 \cdot s \cdot sr$). For the very anisotropic pitch angle distribution of the trapped protons, this will be decreased to about 0.6 $cm^2 \cdot sr$ and the agreement will be poorer. However, the model would not be expected to agree with a single observation to better than a factor of two.

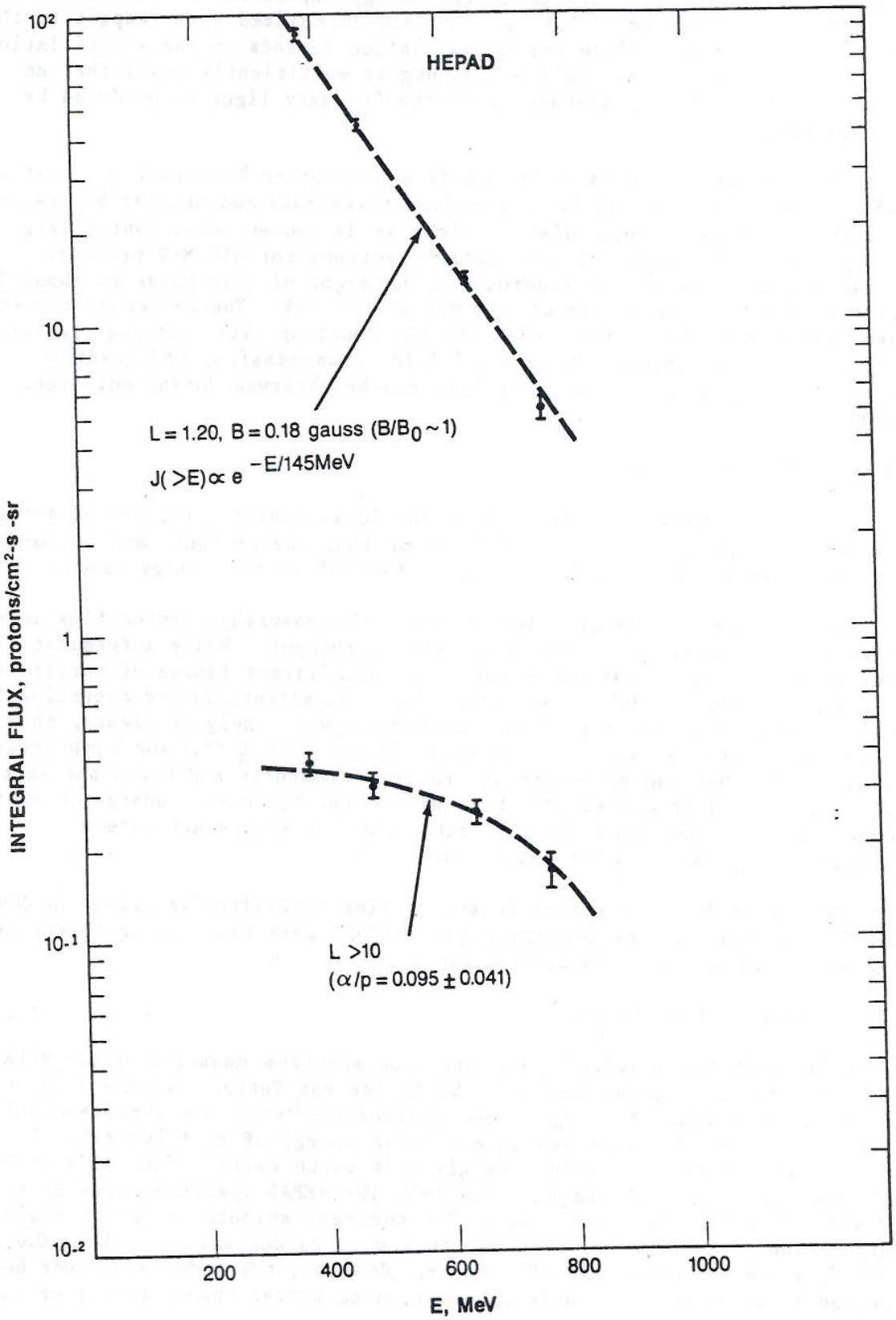

Figure 28.—Comparison of Flux Spectra by Kolasinski

Kolasinski made another check on the performance of the HEPAD using the natural background encountered in orbit. This is of two types: in the polar caps, the galactic cosmic ray background and at low latitudes, the intense inner zone trapped protons. For both types, it is possible to make comparisons with published data. Figure 28 shows Kolasinski's comparison of spectra obtained for these two cases.

To compare to the cosmic ray spectrum, it is necessary to convert to differential flux. For the interval 370-470 MeV, the HEPAD data give 0.061 protons/($cm^2 \cdot s \cdot sr$) which is a differential flux of 6.1×10^{-4} protons/($cm^2 \cdot s \cdot sr \cdot MeV$). For an energy of 400 MeV published values range between 2×10^{-4} and 9×10^{-4} depending on the time in the solar cycle. Thus the agreement is as good as can be expected. Note also that the alpha-to-proton ratio, as shown by (P3 + P4)/(A1 + A2) of 0.095, is reasonable.

6. DATA PROCESSING UNIT (DPU)

6.1 General Description

The Data Processing Unit takes the logic level pulses representing particle events in particular categories and processes them to provide data on the flux and spectrum for telemetering to the ground. In addition the DPU contains the power supplies (DC/DC converter) for the whole SEM and all interfaces with the spacecraft data, command, and power subsystems. The DPU has an analog multiplexer and A/D converter which provide SEM housekeeping data to the TIP data stream. A more limited number of voltages and temperatures are monitored by the Digital B and TIP Analog systems. A view of the unit is shown in Figure 29. A block diagram of the DPU is shown in Figure 30.

In the case of the MEPED and HEPAD data, the DPU operation is an accumulation of the number of events occurring in a fixed time interval. As the dynamic range of the observed flux is very large, the original, accumulated 19-bit number is converted to an 8-bit quasi-floating point representation (p. 61) to reduce the telemetry requirement. The various channels are multiplexed between accumulators and into the telemetry format to provide a sampling rate commensurate with the importance and rate of variation for the particular channel. For the TED data, the DPU carries out the summation over the energy sweep to obtain the total energy and detects the energy interval containing the maximum flux. Alternative telemeter formats (Appendix H) can be selected for the TED data to provide emphasis on different features of the TED submultiplexed data for different application.

6.2 DPU Functions

The DPU performs the following functions:

1. Accumulate pulse outputs from the TED, MEPED, and HEPAD particle detectors and provide count data.

2. Sample analog and digital housekeeping data from the particle

detectors and digitize the analog data to 8 bits.

3. Format the data above into a serial telemetry data stream to the TIROS Information Processor (TIP).

4. Provide analog and digital data from particle detectors and DPU directly to the TIP.

5. Receive, decode, and execute commands.

6. Provide a linear ramp and timing signals for the particle detector in-flight calibrators.

7. Provide power to the particle detectors from a DC/DC converter.

8. The DPU is the SEM interface to the spacecraft.

Appendices D, E and F contain information with cross references on the level sensors and detectors of which the various channels consist.

A block diagram of the DPU appears in Figure 30.

The DPU consists of the following circuits:

a. Timing and Control

b. Analog and Digital Multiplexer

c. Particle Detector Data Processors

d. A/D Converter

e. Formatter

f. Command Processor

g. Ramp Generator and IFC Programmer

h. Low Voltage (LV) Power Supply

a. The Timing and Control receives signals from the spacecraft and uses these signals to generate all the timing signals necessary within the DPU and the three particle detectors. The following timing signals are received by the DPU:

a. 1/32 Hz sync (32 s is a major data frame period)

b. 1 Hz sync

c. 8.32 kHz

d. A1 Select

Signals a and b are used to synchronize with the TIP major frame (32 s) and

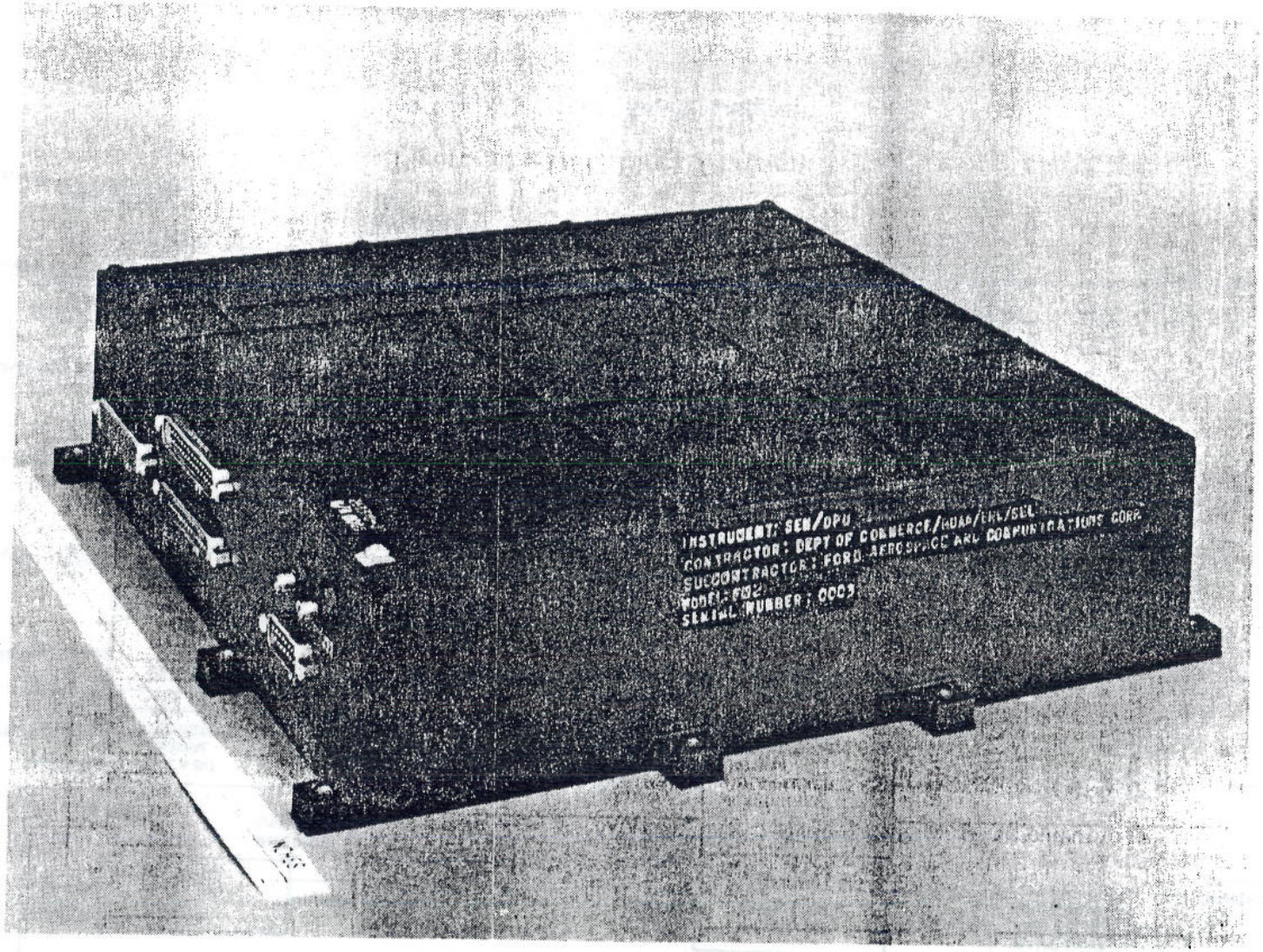

Figure 29.—Data Processing Unit